Radium behaviour in geologic media; application to nuclear waste deposition

Master's thesis

University of Helsinki

Faculty of Science

Department of Chemistry

Otto Tikkanen, B.Sc.

12.5.2020

HELSINGIN YLIOPISTO
HELSINGFORS UNIVERSITET
UNIVERSITY OF HELSINKI
MATEMAATTIS-LUONNONTIETEELLINEN TIEDEKUNTA
MATEMATISK-NATURVETENSKAPLIGA FAKULTETEN
FACULTY OF SCIENCE

Tiedekunta – Fakultet – Faculty	Koulutusohjelma – Utbildningsprogram – Degree programme
Faculty of Science	Degree Programme in Chemistry

Tekijä – Författare – Author
Otto Antti Sebastian Tikkanen

Työn nimi – Arbetets titel – Title
Radium behaviour in geologic media; application to nuclear waste deposition

Työn laji – Arbetets art – Level	Aika – Datum – Month and year	Sivumäärä – Sidoantal – Number of pages
Master's thesis	5/2020	75

Tiivistelmä – Referat – Abstract

The distribution coefficients of radium in Olkiluoto potassium rich biotite were obtained by batch sorption experiments carried out as a function of the concentration of radium and barium. The batch sorption experiments were carried out with four different Olkiluoto associated reference groundwater types: fresh mildly reducing granitic reference groundwater ALLMR (or modified Allard granitic water), glacial anoxic meltwater OLGA, carbonate containing reducing brackish reference groundwater OLBA, and saline reducing reference groundwater OLSR. The main focus of the experiments was to evaluate the effect of the water salinity on the sorption of radium on biotite. The results were compared with sorption results obtained in previous studies done on radium and radium's physicochemical analogue barium.

According to the sorption results, the distribution coefficients of radium on biotite were largest in lower salinity waters. As the barium concentrations of the sorption solutions were increased, the distribution coefficients of radium generally stayed level until they decreased noticeably in the higher studied Ba concentrations (10^{-3} and 10^{-4} mol/l). This suggests that radium is a poor competitor in the ion exchange adsorption interactions on the surface of biotite, when other cations are present in the solution.

As a unique case amongst the more predictable reference groundwaters, the brackish OLBA behaved differently. Despite the increasing salinity of the sorption solutions, the apparent sorption of radium increased steadily throughout the barium isotherm. It was concluded that the high concentration of sulphate in the OLBA reference groundwater caused the occurrence of coprecipitation of radium with the added barium and sulphate as $(Ba,Ra)SO_4$.

Avainsanat – Nyckelord – Keywords
Radium, sorption, deep geological repository, biotite

Säilytyspaikka – Förvaringställe – Where deposited
Kumpulan kampuskirjasto, Helsingin yliopiston kirjallinen arkisto, E-thesis

Muita tietoja – Övriga uppgifter – Additional information

CONTENTS

1 INTRODUCTION **3**

2 BACKGROUND **4**

2.1 NATURALLY OCCURRING RADIUM 7

2.2 OTHER USES OF RADIUM 11

2.3 THE ROLE OF RADIUM IN THE DISPOSAL OF SPENT NUCLEAR FUEL 13

3 CHEMISTRY AND RADIOCHEMISTRY OF RADIUM **15**

3.1 CHEMICAL CHARACTERISTICS 15

3.2 RADIOCHEMICAL ASPECTS 18

4 GEOLOGY OF THE OLKILUOTO DISPOSAL SITE **20**

4.1 OVERVIEW OF LITHOLOGY AND GROUNDWATER 20

4.2 OLKILUOTO-TYPE BIOTITE 22

5 SORPTION OF RADIUM IN MINERALS **24**

5.1 SORPTION AND THE DISTRIBUTION COEFFICIENT 24

5.2 SORPTION OF ELEMENTS IN GEOLOGIC MEDIA 30

6 ANALYTICAL METHODS FOR THE DETERMINING RADIUM **34**

6.1 GAMMA RADIATION MEASUREMENT OF RADIUM 34

6.2 ALPHA MEASUREMENT WITH LIQUID SCINTILLATION COUNTING 37

7 EXPERIMENTAL RESEARCH AND SAMPLE PREPARATION **41**

7.1 BIOTITE 42

7.2 GROUNDWATER SIMULANTS 44

7.3 RADIUM-226 TRACER SOLUTIONS 47

7.4 BARIUM ISOTHERM SOLUTIONS 47

7.5 BATCH SORPTION EXPERIMENTS 48

7.6 GAMMA RADIATION MEASUREMENT AND DISTRIBUTION COEFFICIENT 50

8 RESULTS **52**

8.1 SORPTION PERCENTAGES AND DISTRIBUTION COEFFICIENTS 52

8.1.1 FRESH MILDLY REDUCING GRANITIC GROUNDWATER 53

8.1.2 GLACIAL ANOXIC MELTWATER 55

8.1.3 CARBONATE CONTAINING BRACKISH ANOXIC GROUNDWATER 56

8.1.4 SALINE REDUCING GROUNDWATER 58

8.2 COMPARISON OF RADIUM DISTRIBUTION COEFFICIENTS 60

8.3 DISTRIBUTION COEFFICIENTS IN OTHER RADIUM SORPTION RELEVANT IONS 61

9 DISCUSSION AND CONCLUSIONS 63

9.1 DISCUSSION 63

9.2 CONCLUSIONS AND FUTURE WORK 66

REFERENCES 67

APPENDIX 1 - THE NATURAL DECAY SERIES OF 235U, 238U AND 232Th 74

APPENDIX 2 - THE pH RESULTS OF THE EQUILIBRATED BATCH SORPTION SAMPLES 75

1 INTRODUCTION

According to plans, the highly radioactive spent nuclear fuel from the Finnish nuclear power plants of Olkiluoto and Loviisa will be permanently disposed of in an underground repository facility of ONKALO.[1-5] The repository site lies in close proximity to the Olkiluoto-island nuclear power plant. The process plan is to deposit the nuclear waste deep into the crystalline bedrock in special made iron and copper canisters, and to backfill the deposition tunnels with concrete, swelling bentonite clay, and other materials of very low permeability.[4] The prime principle of the repository facility is to provide multiple barriers, both natural and engineered, to minimize the possibility of escape and further transport of the radionuclides from the designated waste containers.[1] The specially designed fuel canisters are the first retentive barriers, with additional and perhaps the most important protection coming from the surrounding crystalline rock and its radionuclide retentive phases. Thus, the research of the retention of the different radionuclides in the various geologic phases is of paramount importance to the safety analysis of the disposal project.

As uranium is the main component of the spent nuclear waste, its radioactive progeny plays an important role in the safety issue of the nuclear waste disposal. Some radioactive waste safety assessments consider the uranium-238's decay daughter radium-226 to have a notable significance in the safety case dose rate evaluations.[5,6] As a nuclide of some solubility, the migration and sorptive retention of Ra in geologic media in the case of a canister breach or other primary barrier failure must be considered.

In previous studies, it has been assessed that especially the phyllosilicate mica mineral biotite has excellent alkaline earth metal retentive and sorbing qualities.[5,7] Biotite is readily present in the Olkiluoto geosphere as part of the different gneisses.[8] Biotite's role in the retention of Ra has been studied before[7,9] and in addition to this, extensive sorption experiments[10,11] have been carried out on the commonly used analog of Ra; barium. However, as Ra has no stable isotopes

and because of the ensuing challenging radioactive safety issues, the role of Ra itself in these studies has largely been secondary.

The purpose of this study was to provide data in regard to the sorption of ^{226}Ra into geologic media with the focus on biotite and the effect of the salinity of the groundwater with laboratory batch experiments. The sorption was studied with batch sorption experiments in a Ra/Ba isothermic concentration range of 10^{-9} - 10^{-3} M on Olkiluoto-type biotite. Four different types of typical Olkiluoto reference groundwaters were prepared and used in the sorption experiments. All experiments were conducted at room temperature and in oxic conditions.

2 BACKGROUND

In a broad sense, the safety analysis of the Olkiluoto spent nuclear fuel disposal site presents the combined efforts regarding the long-term radiological safety aspects, methodology of researching the designated site's properties, and performance assessments of the repository.[1-5] Specifically it includes a description of the nuclear waste that will be disposed of, the geology of the site, containment procedures, radionuclide release factors and effects on the biosphere in the case of a containment breach, and finally arguments on the reliability of the results on the conducted analyses.[1-3]

The Olkiluoto nuclear waste disposal site is designed according to the KBS-3V method, in which the special spent nuclear waste containment canisters are placed vertically in holes bored into crystalline rock and further surrounded with low permeating materials (Figure 2.1).[1]

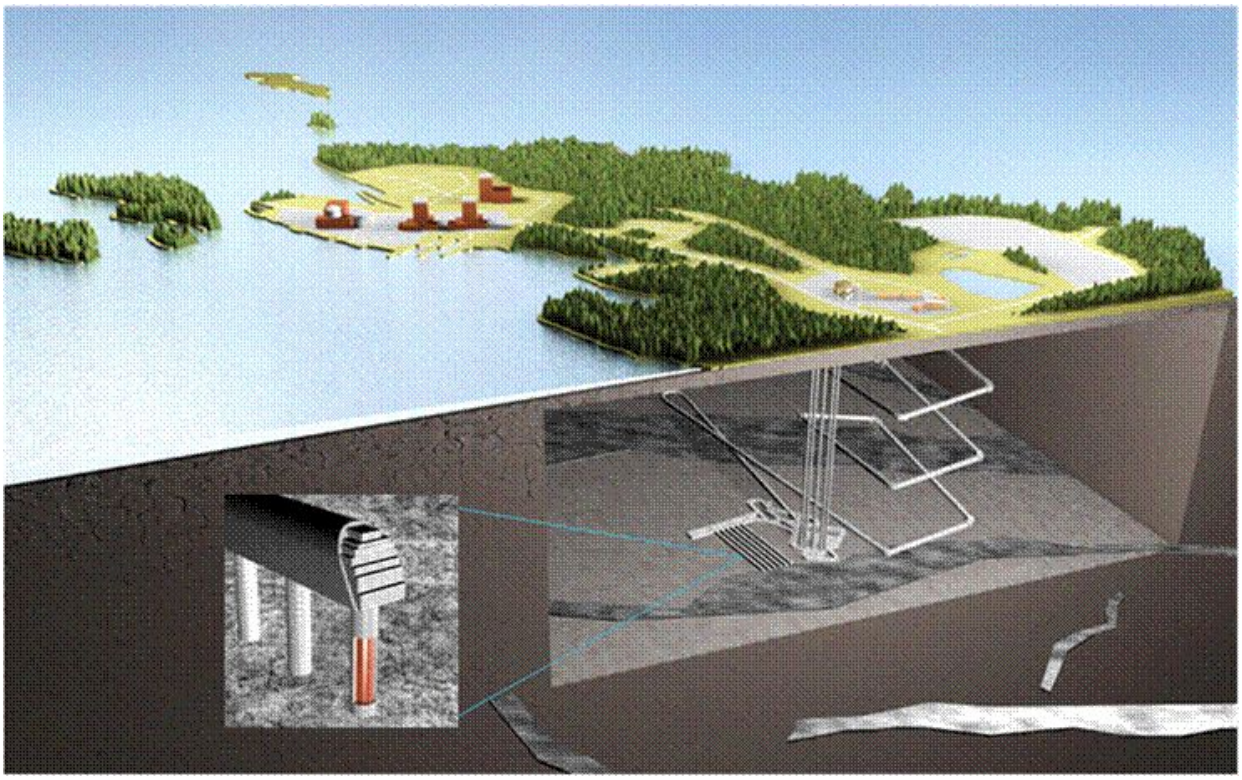

Figure 2.1. A schematic of the KBS-3V disposal method at the Olkiluoto island. Spent nuclear fuel canisters (orange) are placed in underground boreholes. The tunnels are then backfilled after the disposal of the waste canisters. Image modified from Posiva Oy.[1]

The disposing level of the facility is planned to lie between 400 and 450 m below the surface.[1] The geological and hydrogeological properties of the repository tunnel area have been studied and reported on extensively, and have been discovered to be favourable and stable presently and in the future estimations.[5,8,12,13] The Olkiluoto site has been found suitable for long term disposal based on several reasons: stable tectonic situation in the area now and in the foreseeable future, good quality crystalline rock with reducing geochemical properties, and low groundwater flow.[1]

The repository safety case effort includes comprehensive estimations on the behaviour and migration of radionuclides in the solid phase of crystalline rock. These estimations seek to predict the potential radioactive dose on the biosphere in the case of a waste containment breach. To ensure the long-term radiological safety of the repository, especially the nuclides of long half-life and/or high mobility in geosphere have to be considered (Table 2.1).[14]

Table 2.1. Nuclear waste borne safety relevant radionuclides that have long half-lives and/or high mobility in the geosphere. Data from Nummi and group.[14]

Nuclide	Half-life (a)
C-14	5730
Cl-36	301000
Co-60	5.3
Ni-59	75000
Ni-63	100
Se-79	1130000
Sr-90	28.8
Tc-99	213000
Pd-107	6500000
Ag-108m	418
Sn-126	100000
I-129	15700000
Cs-135	2300000
Cs-137	30.1
Pu-238	87.7
Pu-239	24000
Pu-240	6540
Pu-241	14
Pu-242	373000
Am-241	432
Am-242m	141
Am-243	7370
Cm-243	29.1
Cm-244	18.1

Although generally viewed as a low priority radionuclide in radiation safety assessments, ^{226}Ra with its long half-life (1600 a), high radiotoxicity factor, and significant presence, in time, in nuclear waste as being a decay daughter of ^{238}U should still be considered as a notable potential threat to the far-field dose rates and the biosphere.[3,5,6,15,16]

Barium has generally been used as an analogue for Ra, as Ra has no stable isotopes and both elements behave similarly in regard to their chemistry and radiochemistry. However, studies suggest that the chemical similarities of Ba and Ra are insufficient for the sole use of Ba as a substituent for Ra in sorption and general radiochemical behaviour experiments.[7,17] Therefore, it is crucial to provide experimental data of Ra itself to accurately assess its characteristics in geologic media.

2.1 NATURALLY OCCURRING RADIUM

Radium, amongst many other radionuclides, occurs naturally throughout all the environments on Earth.[18,19] The Naturally Occurring Radioactive Materials (NORMs) are most often part of the three decay chains of uranium and thorium (^{235}U, ^{238}U and ^{232}Th, see Appendix 1).[18] Radium's isotopes occur in all three decay chains - ^{226}Ra is a decay daughter of ^{238}U, ^{228}Ra and ^{224}Ra are daughters of ^{232}Th, and finally ^{223}Ra is a daughter of ^{235}U.[18] Of these Ra isotopes, the two with the longest half-lifes, ^{226}Ra and ^{228}Ra with half-lives of 1600 a and 5.75 a, respectively, are also the most abundant isotopes in the Earth's crust and biosphere.[20] Radium-226 is the particularly problematic isotope, as it is widely present in many parts of the world, originating from the U-rich granitic rocks and other acidic rock types.[21] Radium is recognized to be more soluble than U, which promotes its transportation and easier spread in geologic media.[22] Furthermore, there are suggestions concerning the aspect of alpha recoil resulting in the increased desorption of Ra from its host matrix and solution into the surrounding ground water.[18] In addition to this, ^{226}Ra's direct decay daughter radon-222 is a noble gas which can easily emanate from crystalline rock (for example from eskers) and make its way into the air causing local high levels of ^{222}Rn concentration in groundwater and air inside households.[19,23,24]

Although Rn has three naturally occurring isotopes, ^{222}Rn, ^{220}Rn, and ^{219}Rn, the most notable isotope is ^{222}Rn with its half-life of 3.82 days. Multiple reasons affect the high indoor ^{222}Rn concentrations in Finnish houses and buildings: cold climate, construction materials, structure ventilation conventions, and high levels of ^{238}U decay series radionuclides in the soil and bedrock.[19,24,25] In many areas in Finland, heightened levels of ^{226}Ra and ^{222}Rn are found in the drinking water taken from wells outside of the public water supply.[23,24] More than 50 % of the average annual effective dose on Finnish populace is caused by indoor ^{222}Rn and its alpha decay daughters.[26] The health effects caused by the average radioactive dose are difficult to estimate on individuals, but the dose rate provides guidelines on the effect on the health of the general population. Heightened concentration of ^{222}Rn increases the risk of cancer diseases as the gaseous radionuclide is inhaled but decays into less mobile, and much more short-lived daughters (see Appendix 1) before the lung clearance mechanism can evict it.[27]

As a result of increasing health concerns, modern Finnish building regulations take into account the need to limit the concentrations of indoor ^{222}Rn. According to the National Building Code of Finland (B3) and the decision of Finnish Ministry of Social Affairs and Health in 2004, all new buildings are to be designed in such a way that the indoor ^{222}Rn concentration should not exceed 200 Bq/m^3. The National Building Code provides guidelines in the building of ^{222}Rn secure buildings. The Finnish Ministry of Social Affairs and Health has also provided legislation concerning the continuous monitoring of Rn concentration levels in areas of high Rn risk.

Only a fraction of the generated ^{222}Rn in soil and rocks ever leaves the matrix in which it is formed. The escaping part of this is termed the emanation coefficient.[18] Radon-222 levels in buildings are heavily influenced by the physical qualities of the surrounding soil. As Rn is mainly transported via convective flow mechanisms, the permeability and therefore the moisture and coarseness of the soil are important features when studying the incidence of indoor ^{222}Rn. Since soil permeability is often simplified as the examination of the pore sizes of the soil material, it can be assumed that coarse soil and dryness leads to an increase in the ^{222}Rn concentration levels.[18] On the other hand, evidence of the opposite correlation has been found of

^{222}Rn emanation from intact crystalline rock; Hellmuth and group reported that the experimental Rn emanation factor increased with the relative humidity of the Kuru granite samples.[28] The Rn behaviour differences between unconsolidated and compact materials in relation to humidity might be explained with the different modes of transport of Rn in porous soil and crystalline rock. In soil, water acts as a physical hindrance for the outward flow of Rn via airways.[18] Additionally, in soil, the majority of water is detained to the surfaces of large soil grains and does not flow a great deal.[18] In crystalline rock, as the porosity of the material is generally very low and pores are very narrow and intricate, any water in the pore matrix might enhance the mobility of Rn via pore water flow. In addition to this, Rn emanation is further increased in humid (low porous) systems as water absorbs the excess recoil energy of the newly formed Rn atoms, and thus hinders the resorption and retardation of Rn.[18]

Migration of Ra in groundwater can happen through different processes, starting from the weathering of U-rich minerals and to the alpha recoil as the primary source of Ra in groundwater.[29] Uranium (+VI) is easily mobilised as the oxidised uranyl ion (UO_2^{2+}).[29] Uranyl ion is highly soluble and dissolution can lead to near-total solid surface U depletion in certain circumstances.[30] Additionally, U surrounded by carbonate rich waters can form anionic or neutral complexes, which have been reported to be easily transported in soil and rock conditions.[31,32] Although Ra is perceived as the less important species when comparing the mobilisation of Ra and U, as ^{226}Ra is a decay daughter of ^{238}U, the spread of U also contributes to the incidence of Ra in the soil. Despite the low estimated mobility, it has been assessed that 35 % of the Ra in U-rich soils and as high as 40 % of the total Ra in Finnish podzolic soil is easily leachable from the mineral matrix.[19,33] In addition to this, approximately half of the total Ra in soil have been adsorbed as easily exchangeable ions on the surface levels of the soil particles.[19,33,34] This indicates that a large portion of the soil's Ra can be readily transported via various means from the original host rocks to the surface levels of the soil, and even to the vegetation. However, Wagman and group have reported that only the Ra^{2+} ion and $RaSO_4$ have any notable presence in the environment.[35]

An important aspect of Ra migration in the environment is Ra's tendency to coprecipitate with sulphate minerals such as barite, or baryte, ($BaSO_4$) and celestite ($SrSO_4$) as binary solid solutions of (Ba,Ra)SO_4 or (Sr,Ra)SO_4, respectively.[16,36-39] In addition to this, ternary systems of Ra-Ba-Sr-SO_4 have been discovered and studied as well.[38,39] In marine studies, the co-precipitation phenomenon of Ra is well observed and e.g. Ra containing barites accumulated in the deep-sea sediments have been used in paleoceanographic studies.[36] In other surveys relating to the radioactive waste disposal studies, it has been noted that sulphate rich minerals, and especially barite, could be viewed as barrier phases that retard the migration of Ra in the case of a repository containment failure.[16] Langmuir and Riese have estimated that the most important factors when considering the coprecipitation of Ra with barite are the temperature and the degree of non-ideality of the solid solution.[40] It has also been noted that Ra/Ba-ratio in the solid barite is approximately twice of the same ratio in the aqueous solution from which it was formed.[41] Ergo, it can be stated that Ra seems to have some preferential incorporation factor in barite over Ba itself. Despite these preferences in the precipitation processes, the very low natural concentration of Ra makes the existence of pure $RaSO_4$ in nature highly improbable.[16] Hence, it only exists as a part of other minerals.[16,42,43]

Although much of the information concerning Ra is derived from the study of ^{226}Ra, ^{228}Ra as the second-most abundant isotope is present in the soil and rocks, and also in the spent nuclear waste as a product of the radioactive decay of the ^{232}Th decay chain.[44] As ^{228}Ra has a relatively short half-life (5.75 a), even where ^{232}Th is strongly enriched, ^{228}Ra is only present in small trace amounts.[44] Despite this, because of its high decay constant, ^{228}Ra (and ^{224}Ra, to a minor extent) contributes a significant part of the average total Ra specific activity concentrations.[44]

2.2 OTHER USES OF RADIUM

Shortly after its discovery at the end of the 19th century, the use of Ra among other radioactive materials became increasingly popular even in everyday use applications such as bottled drinking water or radioluminous products.[37,44] Additionally, Ra was commonly used in some medical applications, such as brachytherapy.[37] Radium started to be quickly phased out of use in medicine and other commercial products when its inherent (radio)toxicity was discovered in the 1930s. Arriving at the end of the 20th century, Ra was finally replaced with other, safer, radionuclides in medicinal use. Nonetheless, due to the great toxicity and long half-life of Ra, the proper disposal of these formerly used medical instruments has often been neglected.[37] The common procedure has been long-term disposal with other highly radioactive waste in nuclear facilities.[44] Methods for the disposal of Ra from these apparatus have been studied. Today, Ra is mainly used in limited applications in research purposes and Rn measurement standard solutions.[44]

In nature, Ra can leach out of U ore into the surrounding soil via rainwater. The industrial production of Ra is fundamentally similar to this natural 'procedure'. U.S. Nuclear Regulatory Commission describes the production process in the MARLAP instructive manual[45] thus: U-rich ore (or even spent nuclear fuel in some cases) is processed with mineral acids or strong alkali in high temperatures to leach out the U and Ra. After this, Ra can be co-precipitated with Ba as Ba-Ra-SO_4. Subsequently, the sulphates are converted into carbonate form, and Ra is separated from the Ba by fractional crystallization. This process is highly energy and time consuming since the solubility difference between Ra and Ba is minimal. The resulting Ra compound is then amalgamated to form an amalgam of Ra and mercury. Radium is extracted as a pure metal when the amalgam is thermally decomposed in a hydrogen atmosphere.

Radium isotopes in the barite mineral raise a recognized issue in the oil and natural gas drilling industry. The underground liquid and gaseous fossil fuel reservoirs often contain large quantities

of saline water with notable amounts of Ba and Ra dissolved in it.[46,47] The changing physicochemical conditions in the oil and gas during drilling can cause the formation of precipitate sludges in the drilling pipes, tanks, and other equipment. Radium-226/228 activity levels of up to 400 Bq/g have been reported in tank and pipe sludges in some oil fields.[48] The levels are worrisome considering that some portion of the radioactive sludge that is removed from the equipment can end up on the soil surface of the drilling area or adjacent land. Additionally, it has been noted that Ra^{2+} can be released from the barite matrix by some sulphate-reducing bacteria (*Desulfovibrio*).[46] The bacteria dissolve the barite and thus mobilise the Ra in it. Even if the precipitates are carefully collected, radioactive storages are filled up quickly as the industrial action continues.[46]

Uranium mining and milling are among the first steps of the nuclear fuel cycle. Mill tailings are the solid waste minerals that are left behind after the separation of U. Despite rigorous processing, small amounts of U (^{238}U and ^{235}U) and its radioactive progeny, such as ^{226}Ra, are always left in the tailings.[49] These mill tailings are commonly stored as large piles surrounding the mining area.[50] As these tailings are usually stored in outdoor areas, several problems concerning the out-leaching of radioactive materials and other environmentally hazardous compounds due to rainfall or residual acid drainage from ore processing may present themselves in the case of poor storage conditions and a lack of long-term stabilization.[51-54] In several cases, the out-leaching of hazardous materials is hindered with engineered barriers under the designated tailing sites - natural dense clay areas are chosen to be used as tailing sites and other retentive composites are placed under the tailing piles.[49,55] The activity levels of ^{226}Ra have been observed to diminish rapidly in the clay layers under the tailing piles in vertical activity profiles.[49]

According to Boyd, the oldest sites of known Ra contamination predate the discovery of radioactivity.[56] These cases are mostly old mines and other areas of naturally high levels of Ra. Other contaminated sites include the areas of early Ra experiments, most notably those of Ernest Rutherford's experiments and the Curies' research.[56] Before the toxicity of Ra was discovered, the mining, handling, and waste management of Ra-rich materials was careless at best by modern

standards. Even after the discovery of the negative impacts of radioactivity, several contaminated sites have emerged during the era of nuclear weapons testing. Other modern Ra contamination sites include poorly managed U mining areas and some nuclear waste storages.[56] The standard contamination cleaning procedure is the excavation and off-site disposal of the Ra-contaminated soil and material.[56] The contaminated soil and other material are disposed of in special designated radioactive waste storages.

2.3 THE ROLE OF RADIUM IN THE DISPOSAL OF SPENT NUCLEAR FUEL

When designing the nuclear waste disposal system, Ra's behaviour in the retentive barriers has to be taken into account. The Finnish government has issued regulatory requirements concerning the long-term safety and permissible radioactive releases to the environment caused by nuclear repository facilities. Radium-226 as a long-lived alpha emitting nuclide has the annual average release constraint of 0.03 GBq/a.[2] The constraint level of ^{226}Ra is among the strictest when compared to all other discussed radionuclides in the safety report. The Swedish Nuclear Fuel and Waste Management Company (Svensk Kärnbränslehantering AB or SKB) has estimated that Ra will dominate the radiotoxicity levels of the disposed nuclear waste in 500 000 to 1 000 000 years after the closure of the repository.[15,57] Additionally, in many of the estimated KBS-3 multiple canister failure scenarios, both near-field and far-field annual dose rates of ^{226}Ra exceed those that are permissible by safety regulations.[15] This puts a great deal of importance on the stability of the disposal facility and the extreme longevity of the containment canisters.

A great deal of effort and research has been put into the design of the nuclear waste containment canisters.[58] The canisters are designed to be air and water tight, and are able to withstand several hundred millennia worth of corrosion and shear in near-pristine condition. This is necessary in order to ensure that the stored highly toxic nuclear waste does not escape from the containers

into the surrounding geo- and biosphere. The Finnish and Swedish used KBS-3 disposal method containment canister has the following design: a bolt-lidded stainless steel cassette with cast iron insert holes for the spent fuel packages; the cassette is further surrounded by a thick copper jacket with welded or integrated copper lids (Figure 2.2).[58] The copper shell is made of a specially selected copper alloy, Cu-OFP, which has great corrosion resistance and ductility properties to resist the potential damage caused by both chemical weathering and mechanical shear.[58] The spent fuel is placed in the steel cassette's iron inserts as whole fuel assemblies. Several different steel cassette designs exist to accommodate for the multiple types of fuel assemblies used in the different reactor types of the Finnish and Swedish nuclear power plants.

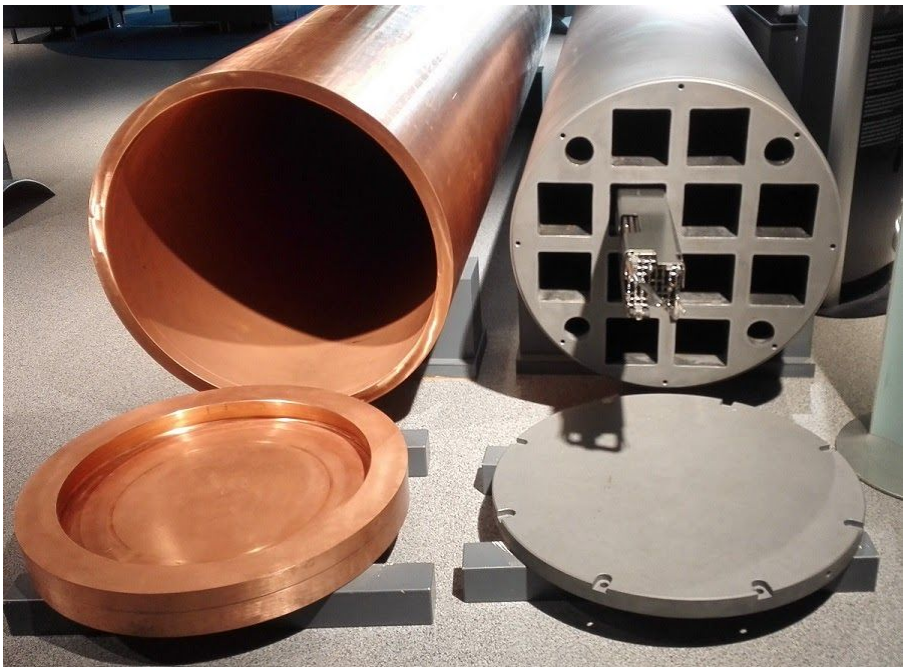

Figure 2.2. A real-size model of the spent nuclear waste containment canister used in the KBS-3 storage method. The diameter of the copper canister is large, 1050 mm. Photo taken by Otto Tikkanen.

The canisters are designed to withstand both external and internal stress. The main objective of the containment canister is to remain leak tight and maintain uncompromised containment for extreme periods of time even when faced with external isostatic pressures of 50 MPa and highly corrosive conditions.[58] The possible internal pressure on the canister assembly has been studied.[59] Internal gas build-up may be the result of corrosion reactions or radioactive decay of the disposed fuel. King and group have claimed, though, that when considering the order of

magnitude of the pressure, the internal stress caused by the pressure is negligible.[59] Additionally, some internal stress may be caused by the heat generated by the decaying nuclear waste between 0 to 50 000 years after the closing of the canister. However, it has been estimated that the internal heat will most likely not compromise the integrity of the containment.[58] Thus, in the case of ^{226}Ra and its progeny, the canisters are expected to be very effective in retarding the escape of said radioactive materials, provided that the containment materials remain pristine.

3 CHEMISTRY AND RADIOCHEMISTRY OF RADIUM

3.1 CHEMICAL CHARACTERISTICS

The group 2 elements in the periodic table are also called alkaline earth metals (Be, Mg, Ca, Sr, Ba, and Ra). They are characterised by having 2 s-orbital electrons in their outer shells and thus they exist mainly in oxidation state +II.[60] In aqueous solutions, they appear as M^{2+} ions. Alkaline earth metals are moderately electropositive and prefer to form ionic bonds with the exception of beryllium, which due to its very small ionic size forms covalent bonds. Ra (Z = 88) is noted as the most electropositive of the group in addition to being characterised with the largest ionic size (Table 3.1). As for its redox properties, Ra exists solely as Ra^{2+} in nature.[60] Most alkaline earth metals readily form hydroxides which are mostly very soluble. Additionally, they often precipitate as moderately soluble carbonates. The largest alkaline earth metals (Sr, Ba, and Ra, Table 3.1) are notable for forming highly insoluble sulphates. Due to their similar physical traits, especially Ra and Ba have comparable chemical properties.[60] Similarly to alkaline metals, alkaline earth metals rarely form coordination complexes with organic compounds as they lack the necessary vacancies in their electron shells.

The large ionic radius of Ra has a direct impact on its chemical properties, such as the thermodynamic aspects and behaviour in aqueous solutions. Due to not having stable isotopes, the determination of Ra's ionic properties has been challenging. A summary of crystal and effective ionic radii of Ra, Ba, and Sr are listed in Table 3.1.

Table 3.1. Crystal and effective ionic radii of Ra, Ba, and Sr. Data from Shannon.[61]

Ion	Coordination number	Crystal ionic radius (Å)	Effective ionic radius (Å)
Ra^{2+}	8	1.62	1.48
Ra^{2+}	12	1.84	1.7
Ba^{2+}	8	1.56	1.42
Ba^{2+}	12	1.75	1.61
Sr^{2+}	8	1.40	1.26
Sr^{2+}	12	1.58	1.44

As can be seen in Table 3.1, the differences between the ionic radii of Ra and Ba are small. The size differences between Ra and Sr are more pronounced. Thus, it is evident that Ra and Ba compounds must share structural similarities. Because of these isostructural properties, Ra co-precipitates with Ba via solid solution formation of $(Ba,Ra)SO_4$ or other compounds such as carbonates.[17] The similarities in ionic radii between alkaline earth metals and also some alkaline metals permits the process of ion exchange between Ra and other ions of analogous ionic radii and charge. It has been noted that ion exchange has a most important role in the retention of radionuclides in the geosphere.[62]

The data on the solubility of Ra is generally very limited, as Ra has no stable isotopes.[17] The physical amount of Ra compounds needed to accurately estimate its thermodynamic properties would often result in radioactivity levels much too high for the modern sense of safe working conditions. Thus, the bulk of the obtainable solubility data of Ra is largely from the beginning of the 20th century,[63] and therefore might not be completely accurate. Despite this, Ra has been

studied to some extent in modern times too, and several readily and sparingly soluble compounds have been discovered and quantified.[17] Table 3.2 lists some very old but still usable solubility data of highly soluble Ra compounds with comparison to corresponding Ba compounds.

Table 3.2. Solubilities of highly soluble Ra compounds in comparison to corresponding Ba compounds in water at 293 K. Data from Erbacher.[63]

Compound	Ionic strength (mol/L)	Solubility (mol/L)	Apparent $\log_{10}$ (K_{sp}^{ap})
$RaCl_2$	2.48	0.83	0.35
$BaCl_2$	5.13	1.71	1.3
$RaBr_2$	5.49	1.83	1.39
$BaBr_2$	10.5	3.5	2.23
$Ra(NO_3)_2$	1.2	0.4	-0.59
$Ba(NO_3)_2$	0.99	0.33	-0.84

As can be seen in Table 3.2, with the exception of $Ra(NO_3)_2$, the solubilities of Ra compounds are lower than the corresponding Ba compounds. This is understood as common behaviour since the solubilities of alkaline earth metal compounds decrease as the element becomes heavier. It is noted that a similar trend should be applicable with nitrate compounds as well, and the exception of $Ra(NO_3)_2$ remains unique among the set.[17] Estimation of the solubility of the sparingly soluble Ra compounds is challenging and results differ depending on the analysis method, but it is commonly realized that the solubilities of Ra sulphates, carbonates and iodates are very low.[17]

Radium is generally viewed as a highly radiotoxic element.[44] It has been noted that the toxicity of Ra in the body depends on the method of exposure. Radium-226 is rarely associated with the inhalation to the lungs, its gaseous decay daughter ^{222}Rn having the dominance in that form of exposure.[44] Following ingestion, Ra is transferred from the gut to the bloodstream. This resorption process is heavily age dependent: the percentage of ingested Ra making its way to the blood varies between as high as 60 % for infants to 20 % for adults.[44] Unabsorbed Ra leaves the body through excretion as feces. Having similar chemical properties as alkaline earth metals to

calcium, Ra has a tendency to accumulate in the skeleton. This is especially problematic since in the skeleton the alpha emitting Ra comes in close contact with the blood cell producing red bone marrow. Long-term effects of Ra ingestion can cause bone inflammation, osteoporosis and bone sarcoma.[44] Considering the release from the skeleton, Ra has a biological half-life of 10 years for adults.[44]

3.2 RADIOCHEMICAL ASPECTS

Radium has no stable isotopes. Radium has four natural isotopes: ^{223}Ra, ^{224}Ra, ^{226}Ra, and ^{228}Ra. Of these isotopes, ^{226}Ra and ^{228}Ra are regarded as the most important, mostly because of their relative abundance in nature as daughters in ^{238}U and ^{232}Th decay series, respectively (see Appendix 1).[60] The most relevant nuclear properties of the natural isotopes of Ra are presented in Table 3.3. As shown in Table 3.3, ^{226}Ra decays into ^{222}Rn. Radon is a gaseous element; in order to reach radioactive equilibrium for the daughters of ^{226}Ra, the Ra source must be hermetically sealed.[24] In such case, the equilibrium for the short-lived daughters (^{222}Rn, ^{218}Po, ^{214}Pb, ^{214}Bi and ^{214}Po) can be reached within a month.[17] Activity of ^{226}Ra is commonly measured with alpha spectrometry[24] (alpha emission of 4874.34 keV with the intensity of 94.038 %) or gamma spectrometry[17] (gamma emission of 186.211 keV with the intensity of 3.555 %). In order to measure the alpha spectrum of ^{226}Ra, it must be separated from its interfering and overlapping alpha emitting decay daughters. Suitable separation methods include evaporation to dryness, coprecipitation, ion exchange and solvent extraction.[7,60] In gamma spectroscopy of ^{226}Ra, one must consider the possible interference of the ^{235}U gamma emission of 185.714 keV when determining the activity of ^{226}Ra from its emission of 186.211 keV.[60]

Table 3.3. Nuclear properties and decay data of the four natural Ra isotopes. Data from Matyskin.[17]

Radium isotope	Half-life	Type of decay	Decay energy (keV)	Decay intensity	Daughters
^{226}Ra	1600 (7) a	α α γ	4874.34 (25) 4601 (1) 186.211 (13)	94.038 (40) 5.95 (4) 3.555 (19)	^{222}Rn, ^{218}Po, ^{214}Pb, ^{214}Bi, ^{214}Po, ^{210}Pb, ^{210}Bi, ^{210}Po, ^{206}Pb
^{228}Ra	5.75 (4) a	X_L γ	14.89645 13.520 (36)	9.6 (19) 1.6 (1)	^{228}Ac, ^{228}Th, ^{224}Ra, ^{220}Rn, ^{216}Po, ^{212}Pb, ^{212}Bi, ^{212}Po, ^{208}Tl, ^{208}Pb
^{224}Ra	3.631 (2) d	α α γ	5685.48 (15) 5448.80 (15) 240.986 (6)	94.73 (5) 5.25 (5) 4.12 (4)	^{220}Rn, ^{216}Po, ^{212}Pb, ^{212}Bi, ^{212}Po, ^{208}Tl, ^{208}Pb
^{223}Ra	11.43 (3) d	α α X_L X_L X_L γ α α X_L γ	5715.84 (21) 5606.99 (21) 83.78 13.6975 81.07 269.463 (10) 5539.43 (21) 5747.14 (21) 94.8547 154.208 (10)	49.6 (12) 25.8 (11) 24.5 (4) 22.1 (4) 14.86 (23) 14.23 (32) 10.6 (10) 10.3 (3) 8.50 (18) 5.84 (13)	^{219}Rn, ^{215}Po, ^{211}Pb, ^{211}Bi, ^{211}Po, ^{207}Tl, ^{207}Pb

Because of Ra and its decay daughter's high biotoxicity, any work with Ra requires extensive safety precautions.[17] All experimental work with Ra should be done in specific protective hot cells or glove boxes. Radium sources should be stored carefully sealed and in stable conditions. As working with ^{226}Ra can release significant amounts of gaseous ^{222}Rn, the used hot cells and

glove boxes should be equipped with ventilation systems to capture any gaseous radionuclides. Dose rates on working personnel should be monitored and external surfaces should be routinely checked for any contaminations.

4 GEOLOGY OF THE OLKILUOTO DISPOSAL SITE

4.1 OVERVIEW OF LITHOLOGY AND GROUNDWATER

Olkiluoto is an island located in the southwestern Finland, on the coast of the Satakunta region near the major cities of Pori and Rauma. Geologically speaking, the Olkiluoto island is located in the Southern Svecofennian complex area,[13] where the land is still rising approximately 6 mm yearly after the last glacial age.[64] The constant postglacial land uplift continually affects the local hydrogeological conditions, but because of the overall stability of the region, these changes in the conditions can be easily projected into the future.[64] As a special geological characteristic of the Olkiluoto area, the effects of the ancient Litorina sea (7500 - 2500 years before present) are still observed in modern times. These effects include the strongly reducing conditions still present on the surfaces of the bedrock. Additionally, a band consisting of heightened levels of sulphates and magnesium has been found at the depth of 100 - 300 m from the surface of the ground.[64]

Olkiluoto's bedrock is generally divided into four main series. The T-series consists mainly of metatexites and diatexites with mica and quartz gneisses and TGG (tonalite-granodiorite-granite) gneisses. These are thought to closely resemble metasedimentary rocks. The S-series which consists of mafic gneisses and quartz gneisses have high levels of Ca originating from the calcareous sediments. The P-series are categorized as granodioritic and tonalitic TGG gneisses

with high levels of phosphorus. The final and the smallest series is characterised as the basic and volcanogenic gneisses, pegmatitic granites, and diabases. The three largest series of T, P and S are estimated to make 42 %, 26 % and 12 % (note that the classifying of the three series may partly overlap), respectively, of the total rock volume of the Olkiluoto island area.[8,13]

During the history of the Baltic Sea, the salinity and overall composition of the seawater has varied with different phases of the glacial retreat. As Olkiluoto is an island surrounded by the sea, the changes in the seawater have, and have had, an effect on its groundwater composition.[65,66] Several distinct layers of groundwater can be identified in Olkiluoto which relate to the historical climatic and shoreline changes of the area.[66] In the Swedish Äspö, a location very much similar to Olkiluoto, it has been estimated that at a depth of around 500 m, the groundwater is mainly a threefold mixture of old meteoric water, old glacial meltwater, and modern Baltic Sea water.[65] Small amounts of ancient isolated highly saline brine exists. It has been noted that Olkiluoto's groundwater has a similar composition.[65,66] According to the safety case geological reports, this type of hydrogeological makeup is considered to be ideal for the purpose of long-term nuclear waste disposal. This is because this type of groundwater system is very stable and is not associated with the active meteoric water circulation. Several adverse effects are associated with construction into underground areas with very high saline groundwater. These effects include the potential corrosion of the construction and/or disposal equipment, decrease of the effectivity of the disposal tunnel back-fill swelling materials, and the decrease of the radionuclide retentive capabilities of the crystalline rock.[65,66] It has been estimated that the retardation of the nuclear waste borne cationic radionuclides (e.g., Sr, Cs, and Ra) are especially dependent on the groundwater salinity and flow properties.[65] The salinity levels of the groundwater have been thought to be low enough on the planned disposal depth of the Olkiluoto repository.[65,66]

Out of the several initially considered disposal facility sites in Finland, Olkiluoto was chosen partly because of the several key reasons in regard to its geological suitability as a long-term repository.[1,5] Perhaps the most important aspect is the current and projected geological stability

of the region. This stability is resultant of the stable tectonic situation, large volume of good quality rock of minor fracturing to build the facility in, low groundwater flows and suitable groundwater salinity conditions, redox conditions suitable for long-term retentive disposal of hazardous radionuclides, and finally the estimated low risk of human intrusion in the future.[1] The disposal site also lies in very close proximity to the Olkiluoto nuclear power plant.

4.2 OLKILUOTO-TYPE BIOTITE

Biotite is a part of the phyllosilicate mica mineral group.[8,67] It consists of negatively charged silicate layers and positively charged interlaying spaces with exchangeable cations holding the layers in place.[8,11] Biotite is defined as a solid solution of potassium or sodium, magnesium or iron, and aluminium containing silicate hydroxide.[8,67] The iron bearing variant of the solid solution is named biotite (alternatively annite or siderophyllite at very high iron concentrations) and its magnesium rich end member is called phlogopite. Olkiluoto biotite has a high level of potassium.[8,67] Biotite is reportedly one of the most common minerals in Finnish crystalline rocks.[8] More specifically, petrology studies from Olkiluoto state that several of the most common rock types there contain significant amounts of biotite.[8] One of the most common rock types in Olkiluoto and Olkiluoto T-series rocks, and the main rock type at the depth of the planned disposal level, is veined gneiss.[8] The average mineral composition of veined gneiss (migmatitic gneiss) is shown in Table 4.1. Biotite is one of the main minerals in veined gneiss, and can even make up to 40 % of the total mass of the rock.[8,67]

Table 4.1. Average mineral composition mass percentage and standard deviation of veined gneiss (migmatitic gneiss). Data from Kärki and Paulamäki.[8]

Mineral	Migmatitic gneiss	
	AVG (%)	STD (%)
Quartz	20.8	12.7
Plagioclase	22.6	16.6
K-feldspar	6.9	8.4
Biotite	20.2	14.3
Muscovite	3.9	5.4
Hornblende	4.1	9.9
Pyroxene	0.1	0.1
Chlorite	3.7	8.3
Cordierite	0.2	0.3
Pinite	5.5	9.9
Garnet	0.1	0.1
Sillimanite	0.1	0.1
Epidote	0.1	0.1
Sphene	0.2	0.4
Apatite	2.1	3.2
Saussurite	2.3	2.8
Sericite	2.0	4.7
Opaques	0.9	1.3

The sorption of radionuclides, e.g. Ba, Sr, and Cs, on Olkiluoto-type biotite has been studied before.[5,7,11] These studies suggest that biotite has strong sorptive properties in regard to earth alkaline metals. Biotite has a high specific surface area and cation exchange capacity when compared to other main minerals of the rocks discussed here.[11] This is facilitated by the special mineralogical structure of biotite: the positively charged cation layer in between the permanently negatively charged silicate sheets provides sites for ion exchange.[68] Since the inner parts of the silicate layers of biotite are thought to be mainly inaccessible, the vast majority of the sorptive processes occur on the broken edges of the sheets, the so-called Frayed Edge Sites (FES).[11] This

special sorptivity makes biotite and biotite containing rocks very good candidates when considering the desired geological aspects of the nuclear waste disposal facility.

5 SORPTION OF RADIUM IN MINERALS

In the case of a containment breach at the spent nuclear waste disposal facility, the first barrier outside of the canister is the back-fill material and the surrounding crystalline rock.[69] As the rock is permeated with flowing groundwater, it is important to try to estimate the water's effect on the migration and retentive aspects of the contaminating radionuclides. The radionuclides have several means of retentive interaction with the water and the rocks and their minerals. These include most importantly the sorption onto different mineral sites, and diffusion through pores and microfractures in the rock matrix.[69]

In this study, as the main focus is placed on the examination of sorption and specifically on ion exchange mechanisms, diffusion is discussed only briefly. Furthermore, as aspects of coprecipitation of Ra have already been discussed in Chapter 3 of this work, they will be forgone for now.

5.1 SORPTION AND THE DISTRIBUTION COEFFICIENT

The term sorption refers to the chemical or physical process where an element or a compound adheres to a sorbing solid surface, out of a solution.[70,71] Sorption processes can occur at the interface of two different phases: liquid and solid, gas and solid, and others.[71] Sorption consists of different physicochemical processes such adsorption (including ion exchange and surface complexation), absorption, and coprecipitation.[71] Sorption and desorption have been

characterised as the most important aspects when considering the overall behaviour and retardation of radionuclides in nature.[70,71]

Adsorption as a term is defined as the process of the adhesion of a solute to a solid surface.[71] It can be divided into two coexisting instances: physical sorption or physisorption, and chemical sorption or chemisorption. Physisorption is caused by the van der Waals' forces which exist between all atoms and molecules.[71] As the van der Waals' forces are the result of fluctuating electron densities thus causing temporal electric dipole moments inside the atoms and molecules, these forces between chemical entities are generally weak. Because of this inherent instability of attraction in the nature of the physisorption itself, these processes are very quick, reversible, and do not much depend on the chemical nature of the participating species.[70,71] However, physisorption is generally thought to be an important form of adsorption for molecules of great length, such as hydrocarbons; each individual atom contributes to the total bond energy between the sorbate and sorbent.[71] Ionic attractions between charged particles of the opposite signs are also included in the concept of physisorption. Chemical sorption, or chemisorption, is a process where the interacting sorbent and sorbate actually form a chemical bond between them. Key characteristics of chemisorption include the property to saturate very quickly all active sorptive surface sites of the solid phase, and the immobilizing aspect of the chemical bond.[71] As a result, in chemisorption the adhesing molecules and ions tend to form a monolayer of contaminants on the sorbent surface. As the forming chemical bonds can be very stable, this form of sorption has the inclination to change the chemical makeup of the solid interface permanently.[71]

Ion exchange is an adsorptive sorption process that is based on the electrochemical interactions between molecules and ions.[70,71] The electric charges on the surface of a sorbing material attract the opposite charges of the surrounding solution's free ions. Thus, ionic complexes are formed between the sorbent and sorbate. As the nature of the ionic charges affects these bonding processes, so, too, do they facilitate the process of ionic exchange itself.[70,71] In the process of ionic exchange, ions compete for the available exchange sites on the interface surface of the sorbent, based on their electronic affinity. Ergo, an ion of higher affinity may have the power to

take the place of a previously sorbed ion of lower affinity.[71] This kind of a process (a binary ion exchange[71]) is illustrated in Figure 5.1, where a cationic exchange sorption takes place between the sorbate interface, lower affinity cations M^+, and a divalent cation R^{++}.

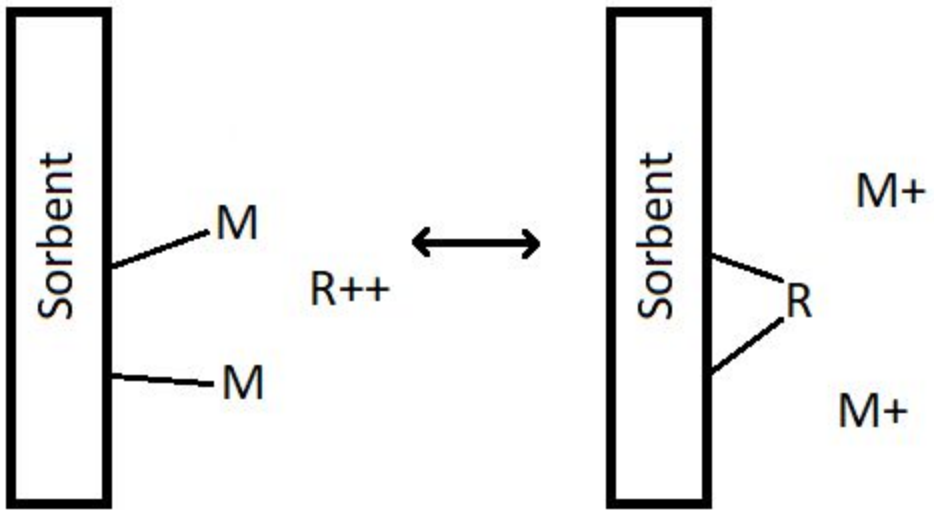

Figure 5.1. A binary cationic exchange sorption where the higher affinity divalent R^{++} ousts the two lower affinity M^+ and is retained to the surface of the sorbate. Should the conditions change, however, the exchange process can be reversible. Artwork by Otto Tikkanen.

In addition to the ionic properties of the sorbate, the overall chemical conditions of the solution and the solid interface affect the process of ionic exchange. As most silicate mineral (e.g. biotite) surfaces in aqueous solutions are commonly described as fronts of hydroxylated metal atoms,[11] it is evident that pH has a considerable effect on the chemistry of sorption. Indeed, at lower pH values the surface sites (≡SOH, where S is a metal atom of the bulk mineral) are protonated ($\equiv SO^+H_2$) and therefore attract more strongly anionic ions.[72] In this case, as per Figure 5.1, the strongly positive R^{++} would be repelled from the solid interface. The situation is naturally the opposite in high pH solutions, as even the mineral surface sites are deprotonated ($\equiv SO^-$) and are much more attracted to the cations of the solution.[72] Subsequently, alkaline earth metal ions, such as Ra^{2+}, are more strongly sorbed in above neutral pH levels. In the case of Olkiluoto, the different types of groundwaters and minerals are generally reported to be mildly basic, and thus very receptive of alkaline earth metals.[7]

The above discussed sorption mechanisms are all part of the overall molecular surface complexation processes. Surface complexation can be divided into two separate types of interactions: inner-sphere complexation, and outer-sphere complexation. Furthermore, these types can manifest as different special cases, such as monodentate or single-bond complexation, and polydentate or multiple-bond complexation. O'Day[72] provides a very good illustration of these types and cases, presented here as Figure 5.2.

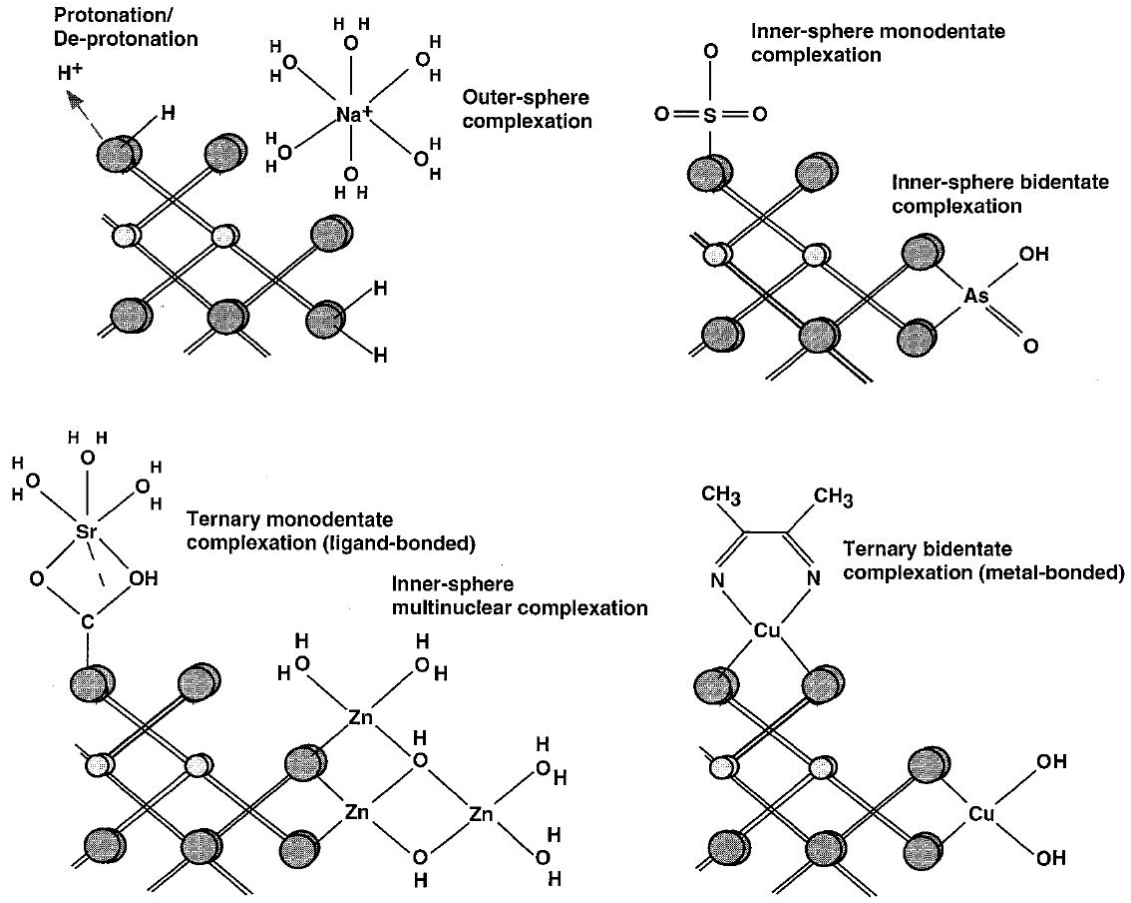

Figure 5.2. Different cases of surface complexation in aqueous solutions. The dark circles represent the mineral surface's oxygen atoms, which are completely hydroxylated. Light circles represent metal atoms of the mineral bulk matrix. Bidentate complexation is the two-bond version of polydentate complexation. Modified from O'Day.[72]

In Figure 5.2, the illustrated outer-sphere complexation can be characterised as the aforementioned physical sorption.[71,72] The sorbate is retained in a hydration sphere by the solid surface but is not actually bonded with it. Ion exchange is a special case of outer-sphere complexation as the sorbate is bound close to the solid surface with electrostatic interactions, but does not form a covalent bond with the sorbent.[71,72] As there is no stable bond between the species, the sorbed ion can easily leave the presence of the solid surface should the chemical conditions of the interface change.[71-73] In the case where the ion is replaced with an ion of higher affinity, it is said that an ion exchange occurs. Because of this instability, the outer-sphere complexation, or ion exchange and physisorption, is thought to be a highly reversible process.[71,72] In contrast to this, the inner-sphere complexation, or chemisorption, is a more stable situation for the participating species, especially for polydentate complexation where multiple bonds are formed between the sorbate and sorbent.[71] Thus, chemisorption can be a highly irreversible and permanent interaction in some cases.

To estimate the sorption affinity of different rocks or minerals in different conditions, the parameter distribution coefficient (K_d in calculations) is often used.[70] The distribution coefficient is an experimentally derived value that reflects the amount of overall sorption occurring in the interaction process of solids and solutions. As discussed above, the actual amount of sorption in a system is heavily dependent on multiple chemical and physical parameters, such as the chemical makeup of the adsorbent surface, the pH, or the concentration and speciation of the contaminants in the solution. So, too, is the distribution coefficient unique to each different situation. As a result, the distribution coefficient has to be calculated for each separate condition. Literary on the subject presents varying derivations and forms of the distribution coefficient formula,[7,60,70,74,75] but in this study the value is calculated based on the equation associated with studies[7,74,75] centered on the general sorption of radionuclides:

$$K_d = \frac{A_i - A_f}{A_f} \times \frac{V}{m} \qquad \text{(Equation 5.1)}$$

where A_i is the activity concentration of the initial aqueous solution before the equilibrium, A_f is the activity concentration of the supernatant solution after equilibration with the solution and sorbent, V is the volume (ml) of the solution, and m is the mass (g) of the sorbent. A more straightforward but less specific value to examine the magnitude of ion specific sorption is the sorption percentage (s%). The sorption percentage represents the amount of activity still left in the solution after equilibrium as a simple ratio to the sample input activity:

$$s\% = 100 - \left(\frac{A_f}{A_i} \times 100\right) \quad \text{(Equation 5.2)}$$

where A_f is the activity of the supernatant solution after the equilibration time between the Ra, water, and biotite, and A_i is the input activity of the sorption system.

As discussed in Chapter 4, even though biotite is one of the most sorptive minerals of the Olkiluoto geology, it is not the sole adsorbent for radionuclides in the bedrock.[5] More than this, the effect of different minerals on whole rock types have to be considered when assessing their affinity for sorptivity. As a consequence of this need for upscaling, conversion factors for the distribution coefficients have been developed to estimate the sorptivity of whole rock types based on their mica mineral content, and the sorptivity on biotite. Ervanne and group present a conversion factor formula for the calculation of sorptivity on intact rock based on values derived from experimental sorption values of crushed rock (biotite),[5] here presented as Equation 5.3:

$$Conversion\,factor = \frac{SS \cdot SUM \cdot Acc}{BET} \quad \text{(Equation 5.3)}$$

where SS is the specific surface area of biotite (0.6675 ± 0.0147 m^2/g, see Chapter 8.1), SUM is sum of mica content in the designated rock type [26.3 % for Olkiluoto T-series mica gneiss (T-MGN), 25.0 % for P-series tonalite granodiorite granite gneiss (P-TGG), 11.5 % for T-series tonalite granodiorite granite gneiss (T-TGG), and 5.3 % for pegmatitic granite (PGR)], Acc is the accessible intact rock inner surface (100 % for T-MGN, T-TGG, and PGR, and 50 % for

P-TGG), and BET is the Specific surface area of the intact rocks (0.9 m^2/g for T-MGN, P-TGG, and T-TGG, and 0.8 m^2/g for PGR). All reported intact rock values are derived from literature.[5] Using Equation 5.3, the sorption conversion values can be calculated for the four different rock types, T-MGN, T-TGG, P-TGG, and PGR (Table 5.1).

Table 5.1. Distribution coefficient conversion factors for various intact Olkiluoto rock types, derived from the specific surface area of biotite.

Rock type	Sorption conversion factor	Conversion factor error
T-MGN	0.195	0.005
T-TGG	0.085	0.002
P-TGG	0.185	0.004
PGR	0.044	0.001

To evaluate the error of the experimental and calculated data, the formula for propagation of uncertainty was used:

$$s_f = \sqrt{\left(\frac{df}{dx} \cdot s_x\right)^2 + \left(\frac{df}{dy} \cdot s_y\right)^2 + \left(\frac{df}{dz} \cdot s_z\right)^2 + \ldots} \qquad \text{(Equation 5.4)}$$

where s_f is the standard deviation of the function f, s_x represents the standard deviation of parameter x, s_y is the standard deviation of y, and so forth.[76]

5.2 SORPTION OF ELEMENTS IN GEOLOGIC MEDIA

Generally in geologic media, sorption occurs most often and most rigorously in materials which have a high affinity to bind and react with the contaminants of the surrounding solutions.[70] High affinity to sorption is a property with many aspects. High sorption usually means high cation

exchange capacity and high specific surface area. Both attributes are often associated with clays.[70] These aspects can be summarized as the chemical makeup of the solid interface and the solution, and the physical form and structure of the solid material.

The sorption of radium has been studied in the past on whole rocks like granite,[77] and clays,[74] on cement,[75] on mica minerals such as biotite,[7] and on goethite and ferrihydrite minerals[78]. Additionally, the sorption of radium analogues Sr, Cs, and most importantly Ba, has been investigated.[7,11] The results tend to share common trends in regard to the behaviour of Ra, or Ra analogues, in geologic systems: Ra is sorbed well in systems with little to no competition between ions in solution, but on larger overall ionic concentrations the amount of sorption stalls and decreases as other more competitive ions saturate the high affinity sorption sites. Indeed, this saturation of the sorption sites results in the decrease of Ra or Ra analogue sorption and the decrease of Ra specific K_d.[7,11,74]

As biotite has been found to be one of the most sorptive minerals of common rock types in Olkiluoto and elsewhere, the sorption processes occurring on biotite-water interface have been investigated and modelled before.[11] Modelling of the adsorptive interactions starts on defining the mineral surface. In previous studies, the surface of phlogopite-biotite was modelled as a standard hydroxylated metal element edge.[11] The sheet like structure of the mica mineral biotite with silicate layers and interlaying cation layers (Figure 5.3) provides sites of high affinity for ion exchange processes.[79]

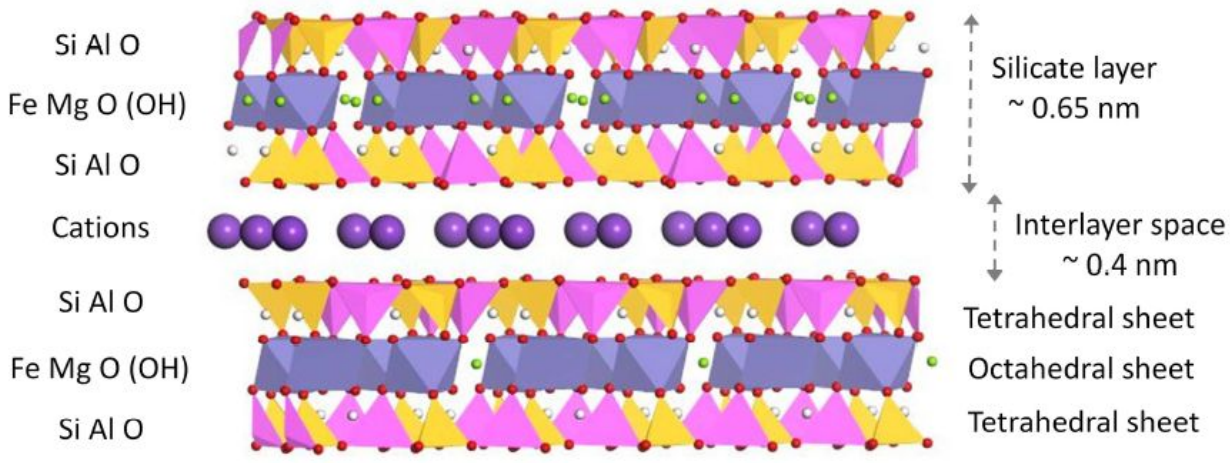

Figure 5.3. The mineral structure of biotite. The structure consists of the negatively charged silicate layer (yellow - Si, red - Al, blue - Fe, and green - Mg) and the positively charged cation layer (purple - K). Modified from Muuri and group.[11]

The cation layer (Interlayer space in Figure 5.3) holds the silicate structure in place and facilitates the ion exchange adsorption. The ends and edges of the sheet-like structure are characterized as sites of high affinity for sorption. These specific spots of ion exchange are called the Frayed Edge Sites (FES), and are estimated to be the most significant contributor to the overall sorption.[11] The aspect of FES in ion exchange is a part of the three site sorption model, created by Bradbury and Baeyens as a result of the examination of Cs sorption on argillaceous rocks.[80] Based on supporting studies, it is presumable that the three site model is also applicable to the sorption of Ba and Ra on biotite.[11,81] Using the three site model, the above-discussed trend of decreasing sorption of the contaminant Ra as the overall salt concentration of the solution increases is explained as the saturation of the high affinity FES, followed by the sorption of Ra onto the far less sorptive Planar and Type II sites.[80]

On the atomic level of sorption on biotite, the aspect of analogy between Ba and Ra might be a more complex matter. Muuri and group provide a comprehensive model of the ion exchange interactions between the K, situated on the edge of a biotite sheet, and the sorbing Cs^{2+} and Ba^{2+} ions.[11] In the model, Ba is an ideal candidate for cation exchange with the interlaying K^{+} ions

(Figure 5.3) owing to its smaller ionic size and bivalent electric charge in comparison to the larger and monocharged K^+. After the sorption of Ba on the very edge of the sheet, it effectively hinders any further ion exchange deeper in the interlayer. According to the model presented in earlier studies, with higher Ba concentrations the edge of the cation interlayer becomes isolated from any further ion exchange between the solution contaminants and the sheet's K.[11] This isolation layer results in the decrease of the amount of FES and thus hinders further sorption. The main difference between Ba and Ra lies most importantly in their ionic size: Ra's effective ionic radius is larger than the same of Ba.[17,61] As a result of this difference, the larger Ra^{2+} might be more sterically hindered to exchange with the interlaying K as opposed to the smaller Ba^{2+}. Consequently, a high concentration of Ba in the solution might affect more the further sorption of Ra than it would with Ba.

In geological systems, diffusion is an important aspect of migration for radionuclides.[70,82] Diffusion is a mechanism which retards the movement of radionuclides with the flow of fracture water. Diffusion is defined as molecular mixing that results from the random Brownian movements of the molecules.[82] If a container with a high concentration of certain molecules is connected to another container with low or zero concentration of the same molecules, given time, the two connected containers will have an equal amount of the molecules in question. A noteworthy trait of diffusion is that it is very slow. Augustithis provides examples of this: HTO spreads in veined gneiss, thanks to diffusion, at a rate of 10^{-13} m^2/s; infinitely diluted Ra^{2+} ion's self diffusion in 25 ^oC water is $8.89 * 10^{-6}$ cm^2/s.[83] Indeed, purely random molecular movement is slow in the commonly thought scale of time. However, thanks to the random movement of molecules resulting from the translational energy, the molecules will spread, in time, evenly to the whole volume of available homogeneous space. This also applies in macroscale situations, such as a nuclear waste container breach releasing radionuclides to the surrounding crystalline rock. If the rock is unfractured and unaltered, and thus has little hydraulic conductivity, the dominating form of radionuclide migration is diffusion.[70,82] As a result, noting the effect of diffusion on the spread of contaminants, e.g. in the case of a canister breach, is of great significance.

6 ANALYTICAL METHODS FOR THE DETERMINING RADIUM

Previous studies on ^{226}Ra have mainly focused on the alpha emission measurement in liquid scintillation counting (LSC) as a method to determine the levels of ^{226}Ra.[7,23] In this form of measurement, the alpha emission of ^{226}Ra with the energy of 4874.34 keV (94.038 %, consult Table 3.3) is examined. However, as the alpha emission of ^{226}Ra is nearly indistinguishable from its radioactive progeny, the samples need to be laboriously processed to separate ^{226}Ra from ^{222}Rn and other alpha emitting radionuclides before any meaningful analysis can be done.[7,60]

In this study, the radioactive measurements of the used ^{226}Ra were conducted on a gamma radiation detector. This method was selected as it requires less tedious sample preparation than liquid scintillation counting to achieve a high level of accuracy and separability of ^{226}Ra. In addition to this, because of the considerably radiotoxic nature of ^{226}Ra and ^{222}Rn, the selected method of simple gamma sample preparation can be viewed as a more safety oriented process than the convoluted alpha sample preparation would be. However, in order to contrast the two analysis methods, liquid scintillation counting is also introduced and discussed in this chapter.

6.1 GAMMA RADIATION MEASUREMENT OF RADIUM

In this study, the gamma radiation of ^{226}Ra (186.211 keV, 3.555 %, Table 3.3) was measured with a semiconductor germanium (Ge) crystal gamma-ray detector to examine the sorption behaviour of radium on biotite. The metrology of gamma radiation has some special considerations to take into account in order to get reliable and accurate results. Gamma-rays are chargeless and do not interact much with, or ionize, the material they pass through.[84] As such,

steps have to be taken in order to maximize the amount of energy absorbed into the detector material from the measured gamma radiation.

Simply put, a Ge or Si crystal gamma-ray detector is a special charged semiconductor with a controlled amount of impurities in it.[84] The semiconductor detector consists of an n-type semiconductor, which is a fine Ge or Si crystal with some contaminant atoms of higher valence number introduced into the matrix. As these contaminants have a higher valence number than Ge and Si, surplus free electrons are present in the crystal. These free electron suppliers are called electron donors. The other part of the detector is a p-type semiconductor, which consists of a Ge or Si crystal with atoms of lower valence number in it. As these contaminants have a lower valence number than Ge and Si, this results in positive electron holes being present in the crystal matrix. These positive electron hole atoms are called electron acceptors. When a strong electric field is applied to the system, a non-conducting depletion region is formed at the interface of the two semiconductors. If the depletion region is disturbed, e.g. with an incoming gamma-ray, the system momentarily becomes conducting and produces a measurable electrical pulse proportional to the energy of the absorbed gamma-ray. This pulse can then be electronically magnified and converted into a digital pulse that can be recorded with a computer.[60,84]

Semiconductor detectors are commonly made of Ge or Si crystals.[60] However, because of their various physical properties, the two different types of detector materials are best suited for different tasks. As Si semiconductors can only manage to produce a narrow depletion zone of less than one millimeter, they are unsuited to measure gamma radiation which is very penetrating due to its chargeless and non-interacting nature.[60] As such, Si detectors are usually employed in alpha emission detection.[60,84] Germanium, with its capability to support a depletion zone of up to several centimeters, is more suited to absorb the elusive gamma-rays.[60] In addition to this, as Ge has a higher atomic number ($Z = 32$) than Si ($Z = 14$), it has a higher tendency to fully absorb gamma-rays and produce photoelectrons which then facilitate the electrical conduction in the semiconductor. This, in turn, results in the Ge semiconductor gamma detectors to have a great energy resolution and accuracy when compared to other forms of gamma radiation detection.[60]

During the early days of Ge detectors in the 1960s, a special manufacturing technique was developed to more effectively control the detection properties of the germanium crystal. As the technology at the time did not allow the growing of sufficiently pure Ge crystals, the depletion zone of the semiconductor was limited to only under a millimeter.[85] This was remedied with the artificial introduction of lithium (Li) atoms to the Ge crystal (Ge(Li) crystal). The Li in the crystal would effectively take the place of other, more detrimental, contaminants in the crystal and compensate for the inefficient ratio of donors and acceptors in the semiconductor. This compensation process of Li in the semiconductor detector material facilitated an unparalleled resolution in gamma radiation detecting.[85] However, a major drawback with the Ge(Li) detectors is the need to constantly cool the detector crystal even when stored, as in room temperature the introduced Li would diffuse through the crystal and unravel the compensation profile.[85]

A newer type of Ge detector, high-purity Ge detector (HPGe), was developed in the 1970s.[85] This type of Ge detector relied on a new technique of producing very high purity Ge detector crystals which could allow a depletion zone of several centimeters. This newfound manufacturing method allowed for larger and more pure Ge crystals to be used in the detectors. In addition to this, as no easily diffusing or reactive materials are used, these detectors can be stored at room temperature. As the detection process requires a rigorous control of the semiconductor's electrical conduction and other properties, the HPGe detectors still would have to be operated at liquid N cooled temperatures (under 110 K). An HPGe detector itself is a high purity Ge diode with contacts made of implanted B and Li.[85] Different types of HPGe detectors are developed, with most common varieties being the p-type and n-type detectors.

6.2 ALPHA MEASUREMENT WITH LIQUID SCINTILLATION COUNTING

Liquid Scintillation Counting (LSC) was developed in the early 1950s to quantitatively measure radiation, and has since been a very popular and widespread method of analysis for radioactive elements from solutions.[60,86] Contributing to the success of the method, LSC can be used to analyse a great variety of types of radiation: alpha, beta (including Auger electrons), gamma (including x-rays), neutrons, and other high energy particles.[86] The basic concept of LSC is that certain aromatic organic molecules have the ability to convert absorbed energy into photons, and that those photons can be measured and used to determine the energy and type of the incident radiation. In practise, a radioactive sample is diluted into a scintillation cocktail, consisting of said radiofluorescent molecules, and then placed into a detector capable of detecting and quantifying the emitted photons. The pulse of light is then amplified and interpreted by the detector apparatus and converted into a digital signal that can be analysed with a computer. In a similar fashion, in solid scintillation a solid crystal (usually NaI) is able to absorb the energy of the incident radiation into its crystalline structure. When this excited state relaxes, the energy is emitted as a photon which can be detected as in LSC.

The sample preparation of LSC has several aspects that need to be considered in order to get good and reliable results. The primary concern is the type of radiation that is to be analysed. Although almost all types of radiation can be measured using special LSC techniques, the method is commonly used to examine sources of alpha and beta radiation.[60,86] Depending on the type of radiation, and also the chemical form of the original sample, a suitable scintillation cocktail has to be selected. Commercially, there exists several types of different scintillation cocktails that are tailored for different situations. Common properties associated and expected of these scintillation cocktails include the need to efficiently transfer the energy of the incident radiation into measurable photons, good efficiency even when the sample-cocktail ratio is not

ideal, good separability and quantifiability of the incident radiation, and low cost.[86] Additionally, important safety factors include low toxicity and high flash point to avoid fire hazard.

Another factor to consider is the material of the sample vessel. Both plastic and glass vials are commercially available. Glass vials have the inherent advantage of transparency. The sample mixture can be visually inspected through the vial wall for any interfering contaminants. In contrast, the plastic vials are less prone to breaking. They are also less expensive and have a tendency to provide a lower background count than glass vials.[86] As a disadvantage, the common polyethylene plastic vials might be permeable when used with types of scintillation cocktails that contain potent organic solvents.[86]

LSC is a manifold process. When a correctly prepared sample containing measurable quantity of radioactivity is placed into an LSC apparatus, the sample is first brought into a light sealed dark detection chamber. The process starts with a radioactive decay of a sample nuclide. As the energy of the radionuclide's decay is emitted as a particle or a wave, it first encounters a liquid scintillation solvent molecule. The solvent molecule then absorbs the incident energy and physically transfers the absorbed energy to a scintillator molecule via intermolecular interactions. During the subsequent deexcitation, the scintillator molecule emits an amount of photons proportional to the energy and type of the incident radiation. In an ideal situation these photons then travel uninterrupted to the photocathodes and photomultiplier tubes (PMT) surrounding the sample vial.[60,86] The photocathodes then register the flashes of light and convert the incoming photons into electrons. After the conversion the electron signal is amplified in the PMTs proportionally to the intensity of the incident flash of light and the amount of electrons released in the photocathode. The final electrical pulse is thus proportional in its magnitude to the original radiation's energy and type.[86] After this, the electrical pulse is further amplified and shaped, and converted into a digital signal that is registered by a multichannel analyser, which sorts the incoming pulses to different energy values based on their pulse height. Finally, the event is recorded in the detector's computer and an energy spectrum can be formed.

To ensure that the detected photon pulse arriving to a PMT is truly from inside the sample vessel, most common liquid scintillation counters employ a system of two connected PMTs.[60] In this system, a final digital signal is recorded only in the case when the two PMTs register the same flash of light. This is called the coincidence mode (Figure 6.1) and it has been developed to lessen the amount of false signals caused by background radiation.[60,87] In this mode, if a true flash of light from the sample occurs, both PMTs receive a photon wave and convert it into an electrical signal. Next, a coincidence module connected to both PMTs checks whether these events happened within a set very narrow time window. Should the two signals have a time separation longer than the set coincident time value, the signals are defined as null and void, and were most probably caused by background radiation. Instead, should the signals be sufficiently simultaneous, they are summed and converted into a digital signal, ready to be recorded in the multichannel analyzer and the detector computer.

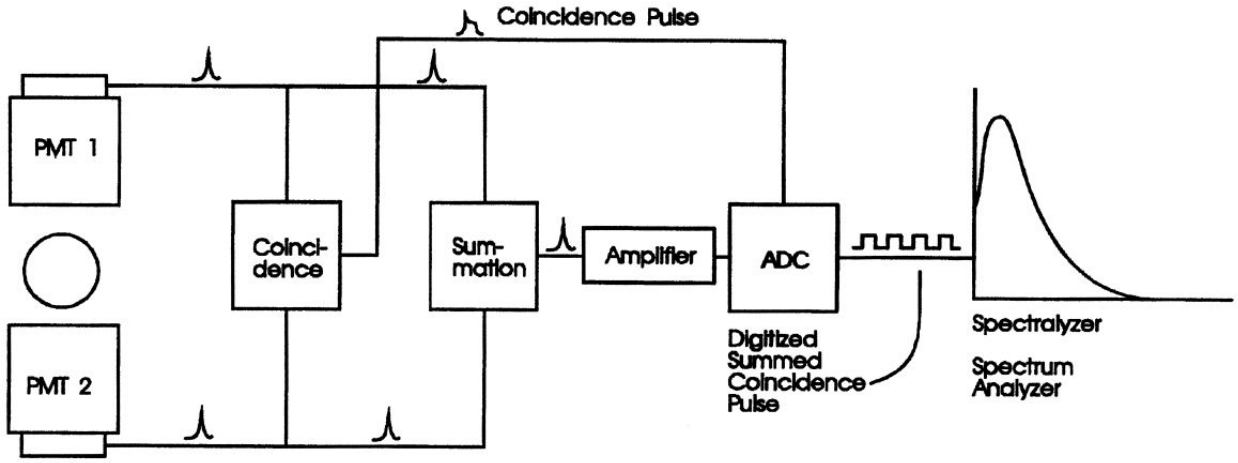

Figure 6.1. A schematic of a liquid scintillation counter with a coincidence module. The coincide mode decreases the amount of false photon detection events and thus lessens the effect of background in the analysis. Image modified from Kessler.[87]

A problematic aspect of LSC is the estimation of efficiency of the measurement.[60,86] The efficiency is a sum of different properties of both the sample and the detector. In the counting process, the effect of quenching has to be taken into account.[86] Quenching is a result of the loss

of energy on the way from the emitted radiation particle to the arrival of the photons to the photocathode in PMT. This loss of energy can be caused, for example, if after the emission the radiation particle loses only a portion of its energy in interactions with other sample molecules before being absorbed by the ideal solvent molecule. In this case the energy measured by the system is smaller than the true energy of the original nuclear decay. This form of quench is called chemical quench. Another form of quenching is the colour quench. In colour quenching, the radiation particle is able to be fully absorbed by a solvent molecule, but part or all of the photons emitted by a scintillator molecule are absorbed by another type of chemical species which normally plays no part in a successful detection of the emitted photons. Once again, in this case the amount of photons finally detected in the PMT are not truly proportional to the full energy of the incident radiation. Ergo, both forms of quench lead to the decrease of the detected energy of the radiation.[86] As quench is always present in LSC to some degree, good efficiency calibrations have to be made before any reliable results are to be gained.[60,86] The effects of quench can be remedied with methods such as the use of internal or external standards, or channel ratio estimations.[86]

LSC is generally considered to be a very good detection method for alpha radiation, and high levels of counting efficiency are most often achieved.[60,86] Despite this, the light conversion of alpha particles based on their energy is interestingly low when compared with beta or gamma radiation.[86] Alpha particles produce scintillation pulses that correspond to approximately one-tenth of the light intensity as beta and gamma radiation of similar energy would produce. In pure alpha emitting samples, this is not necessarily an issue, as no overlapping of the signals can happen. However, this is troublesome with samples that have a mixture of different types of radiation emitters.[86] Because of the low light conversion factor of alpha particles, alpha emissions and beta emissions could overlap in the pulse height spectra even though the alpha particle had ten-fold incident energy when compared to the beta particle.[60] Thus, a need for alpha and beta signal separation is needed.

In modern liquid scintillators, the alpha and beta separation is usually achieved with the focus on the differing properties of signals when produced by an alpha decay event in comparison to a beta decay event.[86] Although alpha particles are known to produce flashes of light much similar in intensity to the lower energy beta particles, the length of those pulses are different.[60,86] Generally, the detected photon pulses produced by alpha particles are tens of nanoseconds longer than the pulses resulting from beta events.[86] This behaviour is due to the longer deexcitation time following an alpha particle absorption.[86] A special discriminator module connected to the scintillator coupling separates the incoming detector pulses to alpha or beta pulses based on their length in time. Ergo, separate spectra of alpha and beta emissions can be formed. This exclusion method is very good for samples that contain radionuclides which produce different kinds of radiation.[60] However, as the photon pulse length is also dependent on the physicochemical properties of the scintillation cocktail and solvents, the α/β-separation factor has to be individually tuned for sample sets that vary in content.[86]

7 EXPERIMENTAL RESEARCH AND SAMPLE PREPARATION

In this study, the distribution coefficients of Ra in biotite in different hydrological conditions were obtained by batch sorption experiments. In these experiments, the overall salinity of the aqueous solutions was examined as a function of the concentration of combined Ra and Ba levels (Ba isotherm). After the batch experiments, estimates of the distribution coefficient values for whole rocks of various common types in Olkiluoto were made. The sorption results were compared with the different types of used waters, with the salinity concentration of the groundwater as a major focus. In addition to this, the experimental results of Ra were compared with previous studies done on other alkaline earth metal radionuclides, such as Ba and Sr.

7.1 BIOTITE

The biotite samples used in this study were prepared from milled biotite originating from Olkiluoto. The biotite was sieved to the grain size of 0.071 - 0.3 mm. As it is important to determine the chemical form of the used biotite to estimate the reliability of the obtained sorption data, the designated biotite had to be purified of any cationic impurities. Olkiluoto biotite is defined as mainly high levels of K containing phlogopite type in the phlogopite-biotite solid solution scale.[67] As such, in the purification the biotite was converted into a mono-potassium form containing only K^+ ions at the ion exchange sites and silicate layer edges.

The following purification process is instructed by Li and group.[88] Approximately 50 grams of milled and sieved biotite was packed into two series connected cation exchange columns of mostly similar properties (Figure 7.1). The biotite and the columns were first washed and the peristaltic pump (ISMATEC High Precision Multichannel Pump) was tested with running MilliQ water through the system for a few hours. After this, a saturated aqueous solution (~ 0.12 M) of purified $KClO_4$ was pumped through the columns for 12 days at a flow rate of 4 mL/h. The waste solution was collected. After 12 days of equilibration, a $KClO_4$ solution of 0.01 M was pumped through the system for two days to equilibrate the K and the biotite with the concentrations of the groundwaters used in the batch experiments. Finally, the columns were washed with MilliQ water for several hours at a high pump flow rate to remove any excess unadsorbed K from the biotite. The purified biotite was then removed from the columns, dried in a vacuum oven at 105 ^oC overnight, weighed, and stored in a sealed vessel until further use.

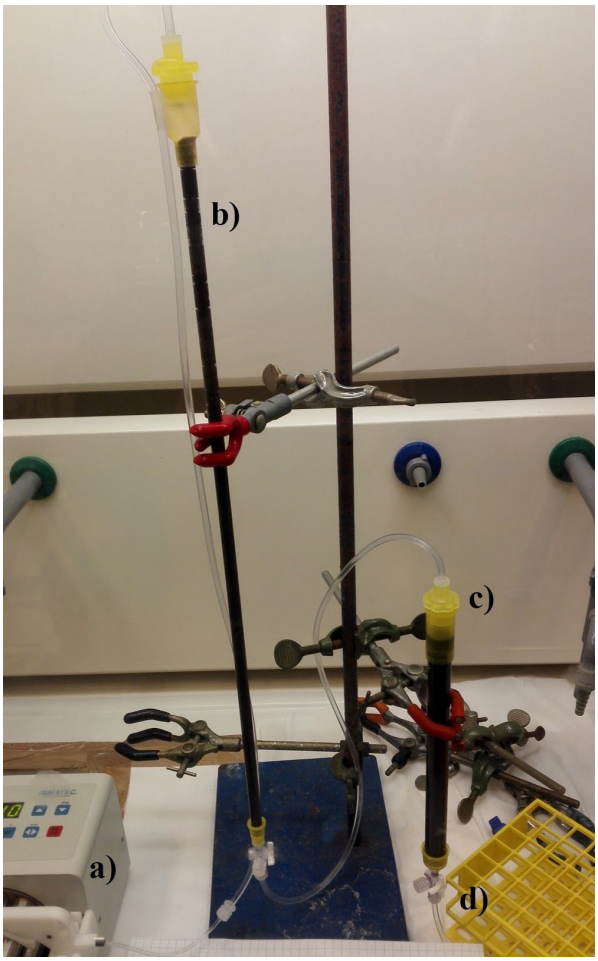

Figure 7.1. The biotite K-conversion setup with a) peristaltic pump connected to b) primary column packed with biotite and c) secondary column packed with biotite, and d) system output tube connected to the waste vessel. Photo taken by Otto Tikkanen.

The mineral purity of the final converted biotite was determined with the XRD method at the Geological Survey of Finland. It was discovered that the analysed biotite indeed was composed mainly of biotite, with minor amounts of other silicates. Examining the crystal structure, it was estimated that the analysed biotite was most likely iron-bearing but Mg rich phlogopite of 1M structure. The next most abundant mineral phase in the analysed sample was clinochlore. Additionally, trace components of quartz, albitic plagioclase feldspar, and microcline were detected. The XRD results are in good agreement with former knowledge on the Olkiluoto biotite.[67] Previous study utilizing the same type of biotite as used in this work reports the biotite's structural formula as $(KMg_{1.76}Fe_{0.7}Ti_{0.54})(Al_{1.08}Si_{2.92}O_{10})(OH_{0.33}F_{0.56}O)$.[89]

The specific surface area (SSA) of the sieved sample was measured with the Brunauer-Emmett-Teller method (BET) at the Chalmers University of Technology, Gothenburg, Sweden. It was determined that the SSA of the converted biotite was 0.6675 ± 0.0147 m^2/g. The obtained SSA result is in sufficiently good agreement with previous studies with similar biotite.[7,11,89]

Cation exchange capacity (CEC) is the measure of negatively charged sites on a solid surface. These negatively charged sites can retard cations. CEC is one of the solid phase values needed in sorption modelling in PHREEQC sorption modelling software. The CEC value of the biotite used in this work has been studied previously: the CEC of the Olkiluoto biotite was determined to be 12.64 ± 0.42 meq/kg.[89]

7.2 GROUNDWATER SIMULANTS

To study the retention of Ra on biotite in different conditions, four different types of groundwater associated with Olkiluoto hydrogeology were chosen. These four waters are described as fresh mildly reducing granitic reference groundwater ALLMR (modified Allard granitic water), glacial anoxic meltwater OLGA, carbonate containing reducing brackish reference groundwater OLBA, and finally the saline reducing reference groundwater OLSR.[4,7] Vuorinen and Snellman[90] further divide the reference groundwaters based on the amount of solids dissolved into them (Total Dissolved Solids or TDS). The types are divided into four categories in Table 7.1.

Table 7.1. The groundwater types are based on the amount of solids dissolved into them. The categorization is based on Vuorinen and Snellman.[90]

Water type	Range of TDS (mg/L)
Fresh water	< 1000
Brackish water	1000 - 10 000
Saline water	10 000 - 100 000
Brine	> 100 000

As per the definition of Table 7.1, ALLMR and OLGA are considered "fresh", OLBA is "brackish", and OLSR is "saline". Brine category is not represented in this study. Groundwaters characterised as types "fresh", "brackish", and "saline" are reportedly found in the planned repository depth of Olkiluoto.[90] Thus, the four selected groundwater types are thought to be representative of the current and estimated future hydrogeological situation in the Olkiluoto disposal facility. All of the used reference groundwaters are characterized as reducing or mildly reducing. By their definition, the ALLMR, OLGA, OLBA, and OLSR are all the anoxic variants of their naturally occurring groundwater counterparts.[90] In this study, however, due to time constraints, special anoxic conditions were not employed during the working phase.

In this study the reference groundwaters were prepared synthetically using analytical grade reagents and MilliQ water as per instructions presented in literature.[4,7,90] Each water was prepared from initially prepared concentrated stock solutions to produce 0.5 L of finished reference groundwater. The final pH of the reference waters were adjusted to correspond to the instructed values with the addition of minimal amounts of 0.1 M HCl and/or 0.1 M NaOH. The recipes of the groundwater preparation are listed below. The used chemicals, their reagent grade, the close approximations of the amounts used in the preparation, pH, and reference ionic strengths of the reference groundwaters are all presented in Table 7.2.

Table 7.2. The chemicals, their reagent grades, and approximate amounts used in the preparation of the Olkiluoto reference groundwaters ALLMR, OLGA, OLBA, and OLSR. Additionally in the table: pH after the solution preparation and the reference ionic strengths from Söderlund and group[7].

Chemical	Reagent grade	Approximate mass concentration after preparation (mg/L)			
		ALLMR	OLGA	OLBA	OLSR
$CaCl_2 * 2 H_2O$	AnalaR NORMAPUR	18.9	2.0	310.1	14672.3
NaCl	puriss p.a.	56.4	1.4	3776.5	12115.8
$MgCl_2 * 6 H_2O$	Baker Analysed	6.0	2.6	221.4	456.6
KCl	pro analysi	7.5	0.9	22.7	39.6
$SrCl_2 * 6 H_2O$	pro analysi	-	-	0.4	106.6
NH_4Cl	pro analysi	-	-	1.0	-
KF	pro analysi	-	-	1.0	-
KBr	AnalaR NORMAPUR	-	-	19.6	-
NaF	purum p.a.	-	-	-	2.7
NaBr	99+%	-	-	-	134.9
KI	AnalaR NORMAPUR	-	-	-	1.2
H_3BO_3	pro analysi	-	-	3.6	5.3
$Na_2SO_4 * 10 H_2O$	pro analysi	28.3	-	1535.7	12.4
K_2SO_4	pro analysi	-	0.8	-	-
$Na_2SiO_3 * 5 H_2O$	purum p.a.	5.6	0.4	-	-
$NaHCO_3$	Baker Analysed	89.6	-	-	-
Set initial pH		8.90	5.79	7.72	8.30
Ionic strength (mmol/L)		4.31	0.123	91.4	515

7.3 RADIUM-226 TRACER SOLUTIONS

Radioactive tracer of ^{226}Ra was purchased from Eckert & Ziegler prior to this study. As the remnants of the first tracer were used during this study, another similar tracer was purchased from Eckert & Ziegler. The tracer solutions, being from the same manufacturer, had similar properties. The initial chemical form of the tracers was reportedly $Ra(NO_3)_2$ in 1 M HNO_3 with 10 μg of Ba per millilitre as carrier. The initial total ^{226}Ra activity of the 5 mL solution was approximately 38 kBq in both solutions. This would make the specific activity of the tracer solution circa 7.6 kBq/mL. Because of the high specific activity and the ensuing radiation safety aspects considering the emanation of ^{222}Rn, before administering the ^{226}Ra into samples, dilutions were made from the raw tracer with MilliQ water. This decreased the specific activity of the used active solutions but facilitated the easier storage of the intermediary ^{226}Ra dilution solutions with having a more manageable total amount of activity in them.

7.4 BARIUM ISOTHERM SOLUTIONS

To study the effect of salinity to the sorption of radium onto biotite, a series of Ba solutions were prepared. Barium was used to tune the concentration isotherm as Ra has no stable isotopes, and evidence suggests that Ba and Ra behave sufficiently similarly in sorption processes due to their chemical similarities (see Chapter 3.1). Barium solutions with concentrations range between 0.1 to 10^{-6} M were prepared using analytical grade $BaCl_2$ (Sigma-Aldrich) and MilliQ water. Calculations were made to estimate the amount and concentration of $BaCl_2$ solution needed to set the Ba/Ra concentration of the sorption samples to desired values.

7.5 BATCH SORPTION EXPERIMENTS

The sorption experiments in this study were conducted mainly using the instructions provided by Söderlund and group.[7] The isotherm batch sorption experiments of the alkaline earth metal Ra were conducted in a ventilated glovebox using 20 mL low diffusion polyethylene (PE) scintillation vials with Al foil sealed screw caps. Approximately 0.5 g of K-converted Olkiluoto biotite was weighed into a sorption vial. After this, the aforementioned four separate Olkiluoto groundwaters (ALLMR, OLGA, OLBA, and OLSR) were added to the separate batches of vials. 10 mLs of specified groundwater was added to each biotite sample. This brought the solid to solution ratio to 50 g/L, similar with previous batch sorption studies.[11] After this, the vials were planned to be agitated for three weeks to equilibrate the biotite with the groundwater, but the uncertainties concerning the availability of ^{226}Ra at that time forced the equilibration time of some samples to extended for up to four months. However, this elongation in the equilibrium time was deemed largely inconsequential in regard to the outcome of the study.

After the first equilibration, the samples were grouped based on the groundwater they held and additionally based on the concentration level of Ra/Ba they were to carry. With each four reference groundwaters, the Ra/Ba concentration isotherm was set to the designated values ($1*10^{-3}$, $1*10^{-4}$, $1*10^{-5}$, $1*10^{-6}$, $1*10^{-7}$, $1*10^{-8}$, and $1*10^{-9}$ mol/l) with the addition of the prepared $BaCl_2$ solutions. Radium-226 dilutions were prepared from the ^{226}Ra tracer solution, and approximately 200 Bq of ^{226}Ra was added to each sample vial. The excess of the dilution solution was sampled to measure with gamma counting to try to estimate the specific ^{226}Ra activity of the dilution solutions. From this specific activity, the actual initial activity of the samples could be calculated. It is noteworthy to state that with the batch with the lowest designed concentration ($1*10^{-9}$ mol/l), the desired isotherm concentration was achieved solely with the amount of ^{226}Ra added. No additional Ba was needed. After the addition of the research solutions, the samples were further agitated for three weeks. During this equilibration, a blanco sample consisting of MilliQ water and 200 Bq of ^{226}Ra was also agitated among the other samples. The blanco

samples were prepared to try to estimate the amount of undesired loss of activity to pipetting, syringe, and/or vial surface adsorption during the processes. Following the second equilibration, the samples were centrifuged at 3000 rpm for 10 minutes (Sigma 3-16KL centrifuge).

In the initial research plan and during the first batches of the sorption samples, the next step after the centrifugation was to pipet 5 mLs of the groundwater supernatant into gamma measurement vials (plastic Al foil screw capped liquid scintillation vials) and proceed to the gamma radiation measurements and calculations. However, during the last four done sorption batches (the concentrations of $1*10^{-3}$, $1*10^{-4}$, $1*10^{-5}$, and $1*10^{-6}$ mol/l) the used radium tracer dilutions were detected to carry irregular amounts of ^{226}Ra in them. The true cause of these irregularities is unknown, but inhomogeneities of the initial ^{226}Ra tracer solution or even undesired ^{226}Ra precipitation as sulphates or carbonates during some of the initial preparation processes are suspected. In practise, this meant that some of the sorption samples held varying and unexpected amounts of ^{226}Ra in them. For some samples it was detected that the actual initial amount of ^{226}Ra was less than 100 Bq, as opposed to the intended 200 Bq. The actual effect of these discrepancies in some ^{226}Ra levels, however, was estimated to be minor as the amount of Ra sorption on biotite was observed to be proportional to the initial Ra levels, rather than an absolute amount of retention that disregards the initial conditions. Regardless, the ^{226}Ra discrepancies do affect the sorption calculations on some level. Ergo, the calculated uncertainties of some of the more badly affected sorption results are bound to be higher than the ones with planned, higher levels of ^{226}Ra.

7.6 GAMMA RADIATION MEASUREMENT AND DISTRIBUTION COEFFICIENT

After the extraction of the groundwater supernatant over the biotite solid phase, the samples were measured with an HPGe gamma-ray detector (Canberra Semiconductor Detector, GX8021) until sufficient statistical confidence of the peak properties was met. The detection data was analysed with Canberra Gamma Acquisition & Analysis software. As the intensity of the ^{226}Ra gamma emission is quite low (3.555 %, Table 3.3) and the percentage of radium sorption on biotite is quite high, meaning that the residual activity in the groundwater supernatant is low, depending on the salinity of the groundwater the gamma measurement counting times varied between a few hours and three or four days. As a rule of thumb, the gamma counting was let to continue until the gamma spectrum analysis software showed the uncertainty of the area of the ^{226}Ra gamma peak to be equal or less than 3.00 %. For example, with a sample of approximately 100 Bq of ^{226}Ra, a sufficient confidence for the gamma peak data is achieved within an hour of measurement. In contrast, for a sample with 5 Bq of ^{226}Ra, the confidence is achieved in no less than two or even three days of measurement. This is perhaps the main disadvantage with the selected gamma measurement method: with the current gamma detection set-up, the sample measurement control is done manually and the counting itself can take extended periods of time depending on the magnitude of the activity in the sample. After the initial experiments, the Minimum Detectable Activity (MDA) of this gamma measurement setup was determined to be approximately 0.5 Bq of ^{226}Ra.

During the gamma measurement, and in general, an airtight sample containing ^{226}Ra emits, in addition to the gamma radiation originating from ^{226}Ra (186.3 keV) itself, gamma radiation from the more prominent gamma emitting decay daughters of ^{226}Ra: ^{214}Pb (242.0 keV, 295.2 keV, and 351.9 keV) and ^{214}Bi (609.3 keV). Some ^{212}Pb (74.8 keV, 77.1 keV, and 238.6 keV), from the decay chain of ^{228}Ra, is also present in all samples. An example of a typical ^{226}Ra gamma spectrum obtained during this work is presented in Figure 7.2.

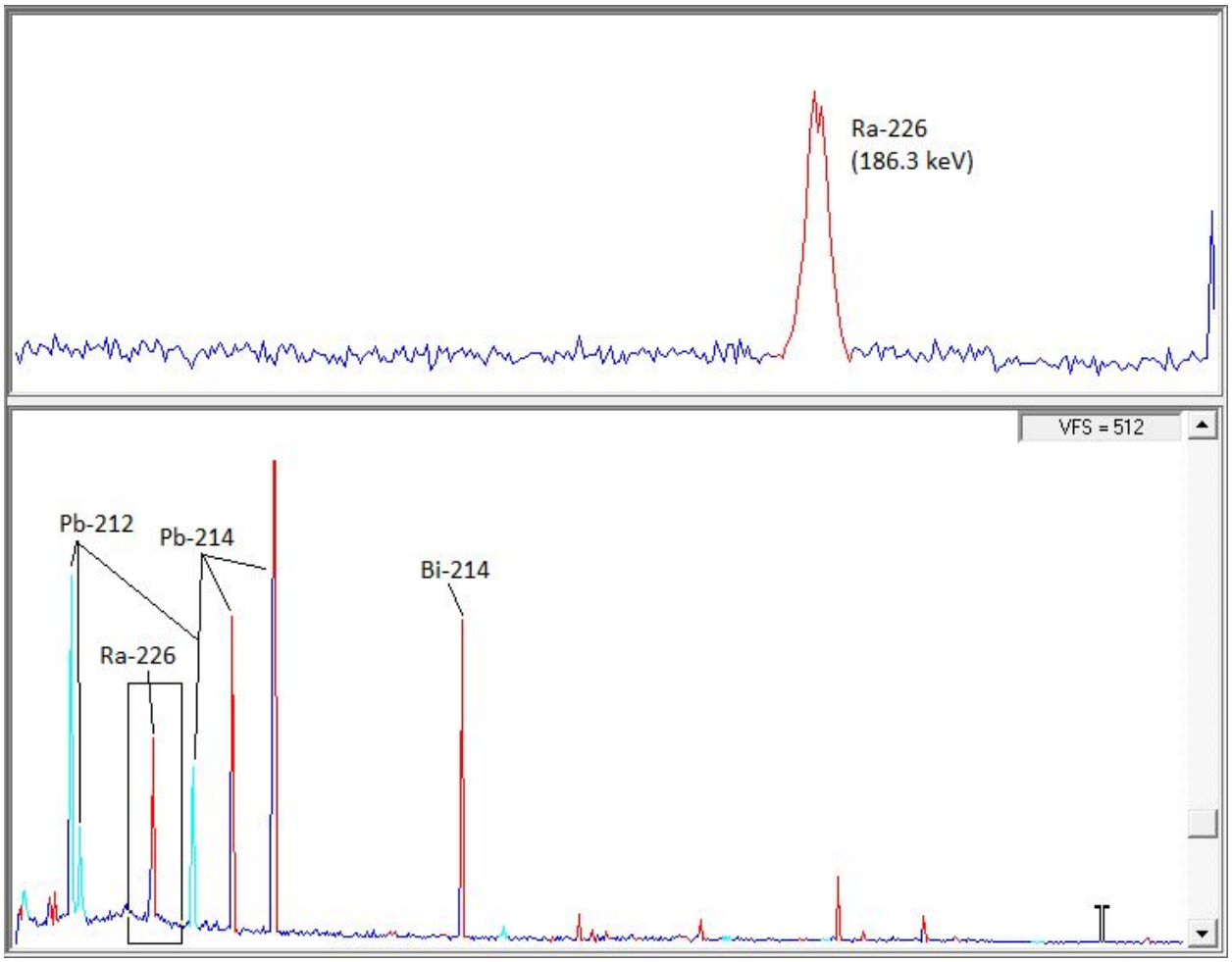

Figure 7.2. (Lower) a typical ^{226}Ra gamma spectrum of this work, as shown in the employed Canberra Gamma Acquisition & Analysis software with the most prominent gamma peaks named therein. In addition to ^{226}Ra, ^{212,214}Pb and ^{214}Bi are also present in most samples. In the upper part of the image, the ^{226}Ra gamma peak of 186.3 keV has been zoomed in to be better visible. Example spectrum provided by Otto Tikkanen.

When the area of the resulting ^{226}Ra gamma peak is calculated, and the gamma measurement time is known, the total activity of the ^{226}Ra in the measured solution can be determined. As the sample vial assemblies were weighed after each addition of solutions during the sample preparation, the total volume of the groundwater solution in the sorption vials can be calculated. Thus, the activity concentration of the sorption supernatant is determined. This knowledge can be combined with the initial activity concentration of ^{226}Ra in the sorption sample (Chapter 7.5) to calculate the distribution coefficient (K_d, Equation 5.1), and the sorption percentage (s%,

Equation 5.2). From radium's distribution coefficients on biotite, using the conversion factors calculated by Equation 5.3 in Table 5.1, K_d values for common Olkiluoto rock types were calculated. Finally, the uncertainties of the results were evaluated with the formula of the propagation of error (Equation 5.4).

8 RESULTS

8.1 SORPTION PERCENTAGES AND DISTRIBUTION COEFFICIENTS

During the sorption experiments, it was discovered that the magnitude of the distribution coefficients of Ra on biotite were quite similar with all of the groundwater types used. A minor exception to this was by the most saline groundwater, OLSR, with which the sorption of Ra was more limited than with the other waters. Thus, the sorption percentages and the distribution coefficients of Ra on biotite with OLSR were notably smaller than with the other tested saline conditions. Additionally, the sorption curves behaved eccentrically with the brackish medium-saline water OLBA. More discussion of this is presented in Chapters 8.1.3 and 9. Notwithstanding, the experimental distribution coefficient results of this study were mostly found to be in quite good agreement with previous batch sorption experiments done with earth alkaline metals on biotite.[7,11]

The sorption percentage and distribution coefficient results are divided into four sections based on the groundwater that was used as the solution in the batch experiment. The results are presented as data points in graphs featuring the magnitude of the Ra/Ba concentration isotherm as the X-axis in logarithmic scale. The presented experimental data points represent the average of triplicate or duplicate sample values and the standard deviation uncertainties are calculated

with the law of propagation of error (Equation 5.4), which takes into account multiple different sources of experimental data error. Additionally, based on the experimental K_d values of Ra on biotite, estimations of K_d values on intact common Olkiluoto rocks are presented with each of the four groundwater types at concentration 10^{-7} mol/l. This is in accordance with the intact whole rock K_d estimation procedure formulated previously.[5] Finally, the Ra K_d results will be briefly summarised and compared with other sorption correlating ions in Chapters 8.2 and 8.3.

The pH values of the samples were measured at the equilibrium of Ra, the groundwater, and the biotite. The pH results of the batch sorptions in different concentrations for each of the four groundwater types are presented in Appendix 2.

8.1.1 FRESH MILDLY REDUCING GRANITIC GROUNDWATER

Modified Allard reference groundwater, or ALLMR, is described as 'fresh mildly reducing granitic' reference groundwater.[7] As presented in Table 7.2, ALLMR has only a moderate amount of dissolved salts in it. As discussed in Chapters 3 and 5, and as shown in relevant literature,[7,11] the low salinity of the groundwater in batch sorption experiments would predict a high amount of Ra sorption onto the biotite adsorbent. Indeed, as shown in Figure 8.1, the sorption percentage of Ra is consistently high through the Ra/Ba concentration isotherm, only showing the predicted signs of reducing in the most Ba concentrated solutions of 10^{-4} and 10^{-3} mol/l. This high percentage of sorption reflects to the distribution coefficient (K_d) values as well, and thus the values stay high until the more concentrated solutions.

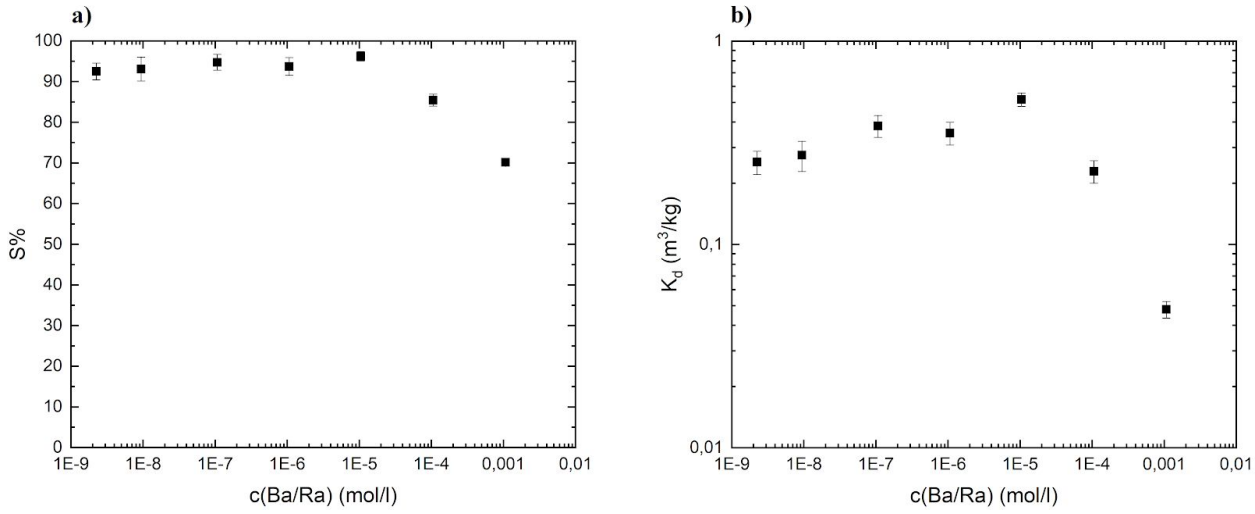

Figure 8.1. The batch sorption results a) as sorption percentages and b) as distribution coefficients of Ra on biotite as a function of Ra and Ba concentration isotherm in ALLMR reference groundwater. All data points are presented as an average of triplicate or duplicate samples, and the uncertainties of the points are presented as one standard deviation of mean calculated with the law of propagation of error.

As biotite is an important part of several of the most common Olkiluoto rock types, a conversion of Ra K_d values on crushed rock (biotite) to Ra K_d values on intact rock can be made with the conversion values presented in Table 5.1. The estimate of Ra K_d values on some intact rocks in ALLMR conditions with the Ra/Ba concentration of 10^{-7} mol/l are presented in Table 8.1. The K_d value of Ra on biotite in the Ra/Ba concentration of 10^{-7} mol/l was calculated to be $(3.8 \pm 0.5) * 10^{-1}$ m^3/kg.

Table 8.1. Estimates of Ra Kd values and uncertainties on some intact whole rocks of Olkiluoto in ALLMR conditions of Ba/Ra concentration of 10^{-7} mol/l.

Type of intact rock	Kd (m^3/kg)
T-MGN	(7.5±1.0)E-02
T-TGG	(3.3±0.5)E-02
P-TGG	(7.1±0.9)E-02
PGR	(1.7±0.3)E-02

8.1.2 GLACIAL ANOXIC MELTWATER

The Ra on biotite sorption results of the glacial anoxic meltwater reference groundwater OLGA are presented in Figure 8.2.

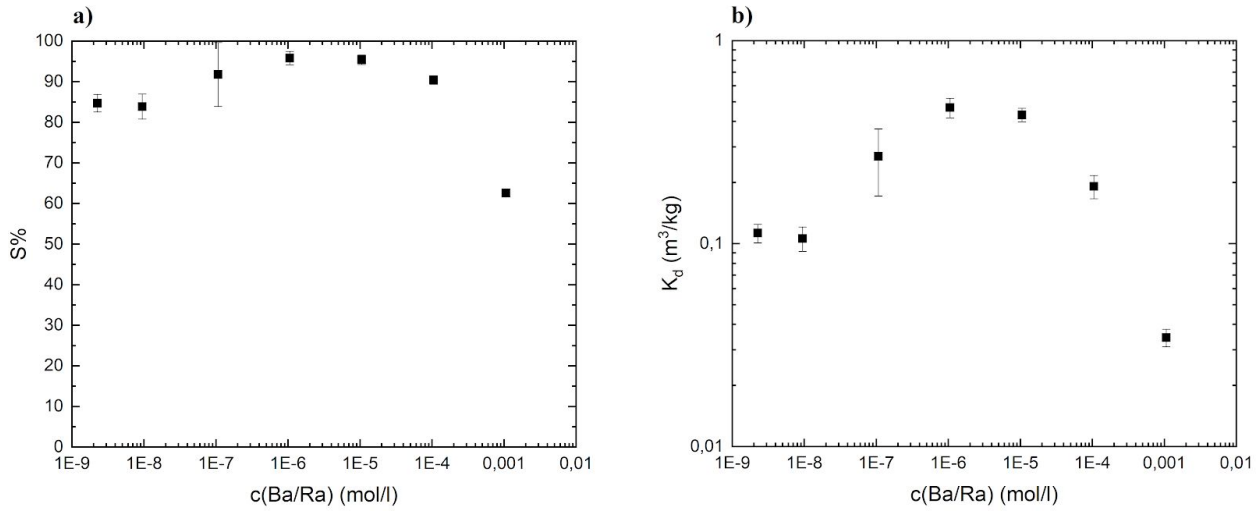

Figure 8.2. The batch sorption results a) as sorption percentages and b) as distribution coefficients of Ra on biotite as a function of Ra and Ba concentration isotherm in OLGA reference groundwater. All data points are presented as an average of triplicate or duplicate samples, and the uncertainties of the points are presented as one standard deviation of mean calculated with the law of propagation of error.

OLGA is characterised as a glacial anoxic meltwater.[7] Because it simulates the fresh meltwater of a glacier, it has very little dissolved salt in it. This, in turn, facilitates a high magnitude of Ra sorption onto biotite. In practise, this meant that very little amount of Ra was left in the sorption supernatant after Ra and biotite equilibration. This, in turn, made the gamma measurement of Ra more challenging, and might have played a part in the suspicious bump of the K_d trend between Ra/Ba concentrations of 10^{-7} and 10^{-4} mol/l.

The estimates of Ra K_d values on some intact rocks in OLGA conditions with the Ra/Ba concentration of 10^{-7} mol/l are presented in Table 8.2. The K_d value of Ra on biotite in the Ra/Ba concentration of 10^{-7} mol/l was calculated to be $(2.7 \pm 1.0) * 10^{-1}$ m^3/kg.

Table 8.2. Estimates of Ra Kd values and uncertainties on some intact whole rocks of Olkiluoto in OLGA conditions of Ba/Ra concentration of 10^{-7} mol/l.

Type of intact rock	Kd (m^3/kg)
T-MGN	(5.3±2.0)E-02
T-TGG	(2.3±0.9)E-02
P-TGG	(5.0±1.9)E-02
PGR	(1.2±0.5)E-02

8.1.3 CARBONATE CONTAINING BRACKISH ANOXIC GROUNDWATER

OLBA is described as a carbonate containing brackish anoxic reference groundwater.[7] OLBA represents the middle point in the groundwater salinity comparison as it has notable amounts of sodium and chloride in it, approximately 1800 and 2500 mg/l, respectively. Since the setting of the Ba isotherm was made with $BaCl_2$ solutions, the amount of Cl^- in the more concentrated Ra/Ba conditions is even higher. The Ra on biotite sorption results of OLBA groundwater are presented in Figure 8.3.

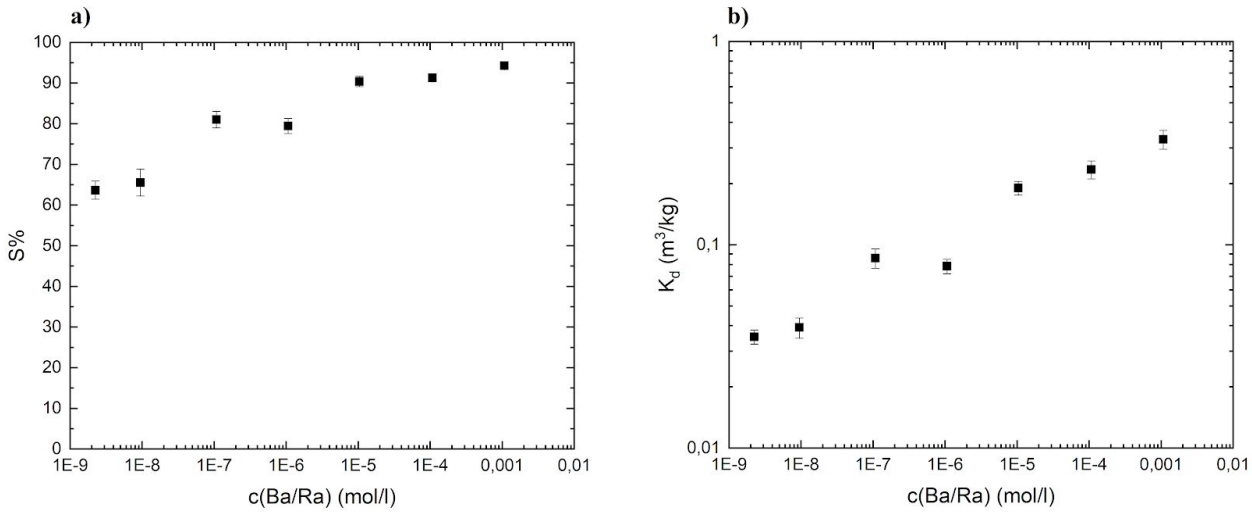

Figure 8.3. The batch sorption results a) as sorption percentages and b) as distribution coefficients of Ra on biotite as a function of Ra and Ba concentration isotherm in OLBA reference groundwater. All data points are presented as an average of triplicate or duplicate samples, and the uncertainties of the points are presented as one standard deviation of mean calculated with the law of propagation of error.

Unique amongst the waters of this study, OLBA contains a considerable amount of sulphate: 458 mg/l, which is a fiftyfold increase in comparison to ALLMR and OLSR (Table 7.2). The higher sulphate concentration might explain the abnormality in the sorption percentage and distribution coefficient trend, as against predictions the sorption of Ra onto biotite in OLBA keeps increasing as Ra/Ba gets more concentrated in the solutions. The high amount of sulphate and Ba in the solution might result in Ba precipitating as BaSO4 during the equilibration period. As discussed by Matyskin, Ra has a tendency to co-precipitate with Ba as $(Ba,Ra)SO_4$.[17] This co-precipitation would, in effect, retain some of the Ra in the solid phase of the sample, not adsorbed but as a precipitate. Despite this distinction, the chosen Ra sorption measurement method of this study would imply an increased amount of sorbed Ra on biotite, thus distorting and increasing the apparent sorption percentage and K_d of the condition. This co-precipitation is most likely unique to OLBA, as the other used reference groundwaters contain only a small fraction of the sulphate that OLBA contains.

The estimates of Ra K_d values on some intact rocks in OLBA conditions with the Ra/Ba concentration of 10^{-7} mol/l are presented in Table 8.3. The K_d value of Ra on biotite in the Ra/Ba concentration of 10^{-7} mol/l was calculated to be $(8.6 \pm 1.0) * 10^{-2}$ m^3/kg.

Table 8.3. Estimates of Ra Kd values and uncertainties on some intact whole rocks of Olkiluoto in OLBA conditions of Ba/Ra concentration of 10^{-7} mol/l.

Type of intact rock	Kd (m^3/kg)
T-MGN	(1.7±0.2)E-02
T-TGG	(7.3±0.9)E-03
P-TGG	(1.6±0.2)E-02
PGR	(3.8±0.5)E-03

8.1.4 SALINE REDUCING GROUNDWATER

OLSR, or the saline reducing groundwater,[7] is the most saline of the reference groundwater types used in this study. OLSR contains high amounts of Na^+, Ca^{2+}, and Cl^-, approximately 4800, 4000, and 14500 mg/l, respectively. Similarly to other groundwaters, in the sorption experiments the Ra/Ba concentration was set with $BaCl_2$, so the amount of Cl^- is even higher than the reference groundwater recipe states. Additionally, it contains approximately 35 mg/l of Sr^{2+}, which has been assessed to be one the major competitors of Ra^{2+} in ion exchange adsorption processes.[7,11,17] The high salinity of OLSR thus hinders the sorption of Ra as the solution has a high amount of ions competing for the adsorption sites on biotite. This is evident of the batch sorption results (Figure 8.4), in which the experimental K_d values start at one tenth of the other reference waters' comparable values. The sorption percentages of Ra on biotite in OLSR are approximately half of the sorption percentages of other waters.

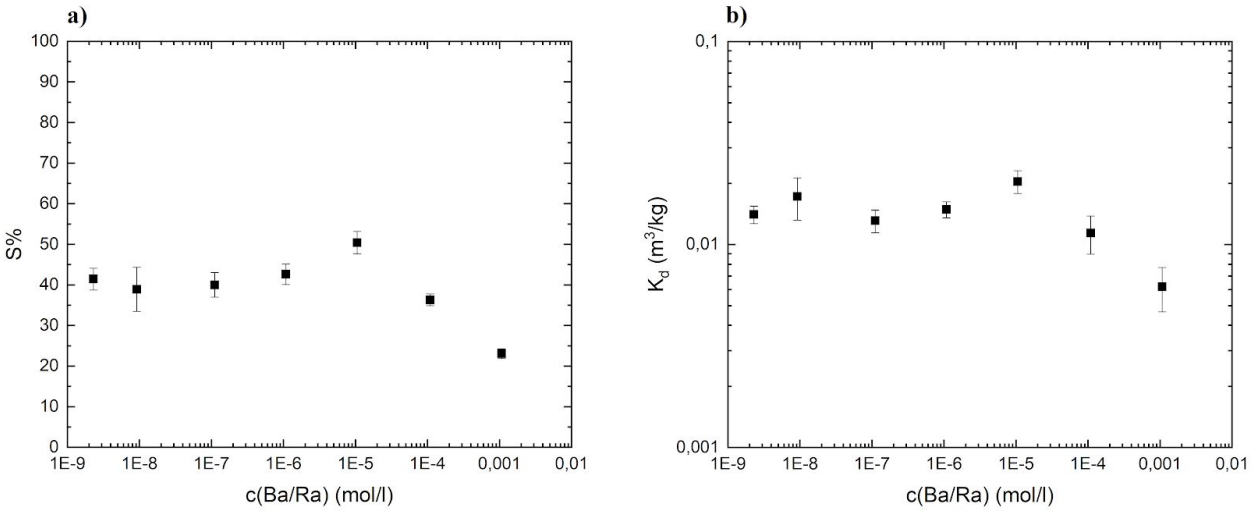

Figure 8.4. The batch sorption results a) as sorption percentages and b) as distribution coefficients of Ra on biotite as a function of Ra and Ba concentration isotherm in OLSR reference groundwater. All data points are presented as an average of triplicate or duplicate samples, and the uncertainties of the points are presented as one standard deviation of mean calculated with the law of propagation of error.

The estimates of Ra K_d values on some intact rocks in OLBA conditions with the Ba/Ra concentration of 10^{-7} mol/l are presented in Table 8.4. The K_d value of Ra on biotite in the Ra/Ba concentration of 10^{-7} mol/l was calculated to be $(1.3 \pm 0.2) * 10^{-2}$ m^3/kg.

Table 8.4. Estimates of Ra Kd values and uncertainties on some intact whole rocks of Olkiluoto in OLSR conditions of Ba/Ra concentration of 10^{-7} mol/l.

Type of intact rock	Kd (m^3/kg)
T-MGN	(2.6±0.4)E-03
T-TGG	(1.1±0.2)E-03
P-TGG	(2.4±0.4)E-03
PGR	(5.8±0.8)E-04

8.2 COMPARISON OF RADIUM DISTRIBUTION COEFFICIENTS

To illustrate the varying nature of the Ra sorption trends of the studied reference groundwaters, all of the above presented Ra on biotite distribution coefficient results are further collected into Figure 8.5. The decrease of Ra sorption in higher Ra/Ba concentrations is most evident in ALLMR and OLGA, and to a minor degree in OLSR. OLBA forms the exception to this expectation, as the Ra sorption seems to be increasing even with higher Ra/Ba isotherm concentrations.

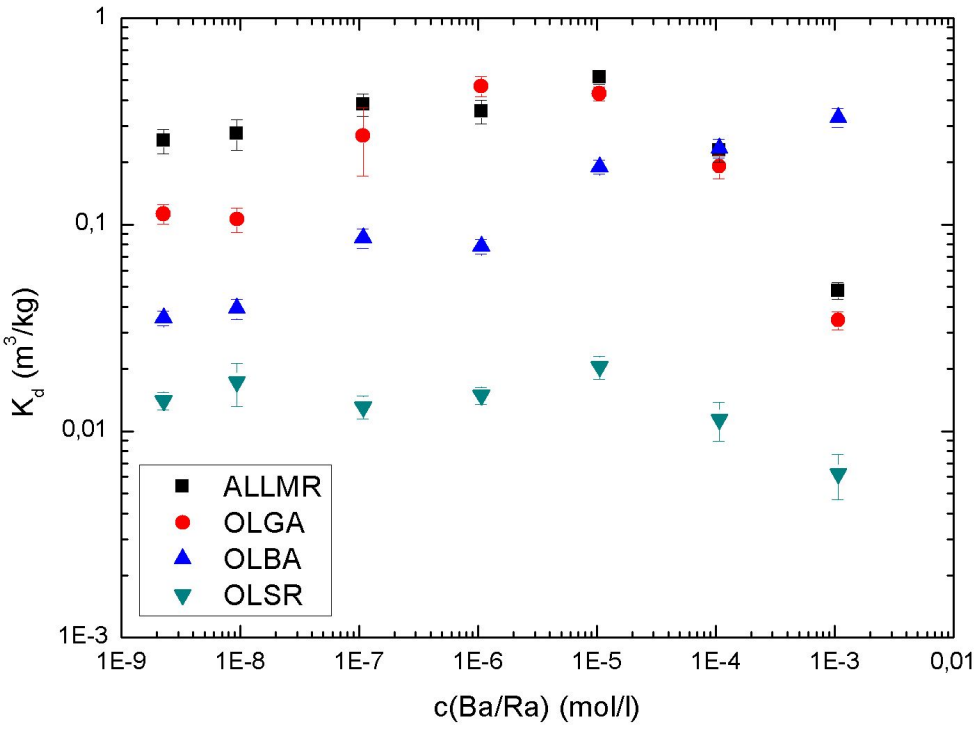

Figure 8.5. The batch sorption results as distribution coefficients of Ra on biotite as a function of Ra and Ba concentration isotherm in ALLMR, OLGA, OLBA, and OLSR reference groundwaters. All data points are presented as an average of triplicate or duplicate samples, and the uncertainties of the points are presented as one standard deviation of mean calculated with the law of propagation of error.

8.3 DISTRIBUTION COEFFICIENTS IN OTHER RADIUM SORPTION RELEVANT IONS

In previous sorption studies, it has been assessed that the sorption of Ra on biotite and crystalline rock shows some correlation with other ions than just the most physicochemically similar Sr^{2+} and Ba^{2+}.[7,91] Most notably these ions include Na^{+}, Ca^{2+}, and Cl^{-}. To highlight the correlation between the Ra sorption and the concentration of the above mentioned ions in the different studied reference groundwaters, the batch sorption results of Ra as distribution coefficients are presented as functions of the ion concentrations in the reference groundwaters in Figure 8.6. To more easily compare the data, the Ra/Ba isotherm concentration of 10^{-7} mol/l was chosen as the point of focus for the reference groundwaters. The magnitude of the Cl^{-} ion concentration originating from the added $BaCl_2$ as a part of the Ra/Ba isotherm setting is negligible in the chosen Cl^{-} concentrations.

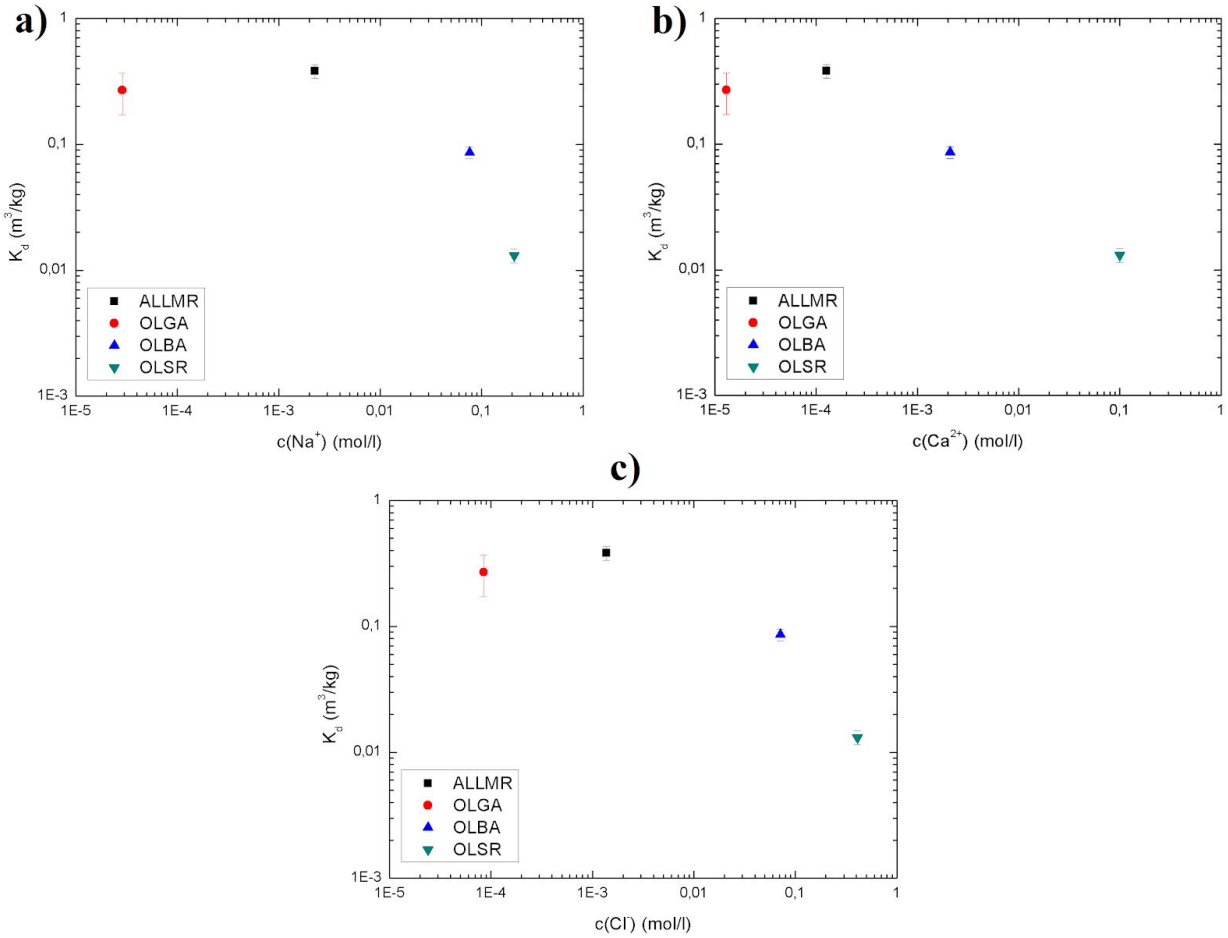

Figure 8.6. The batch sorption results as distribution coefficients of Ra on biotite as a function of a) Na^+ b) Ca^{2+} and c) Cl^- concentration in Ra/Ba isotherm concentration of 10^{-7} mol/l ALLMR, OLGA, OLBA, and OLSR reference groundwaters. All data points are presented as an average of triplicate or duplicate samples, and the uncertainties of the points are presented as one standard deviation of mean calculated with the law of propagation of error.

9 DISCUSSION AND CONCLUSIONS

9.1 DISCUSSION

As was initially predicted, based on previous sorption studies of Ra and Ra analogues, in this study the least amount of Ra sorption on biotite occurred with the most saline water of OLSR (Figures 8.4). This, in turn, was reflected upon the distribution coefficient values in OLSR, which were only a tenth of the corresponding values in the fresh groundwater of OLGA (Figure 8.2). The sorption percentage of Ra in OLSR was constantly approximately half of the sorption percentage values of the fresh OLGA. Thus, the distribution coefficients of OLSR are generally one order of magnitude lower than with the more fresh waters (Figure 8.5). This tendency for a smaller amount of sorption in the more saline water can be explained with the increasing competition between the ions of the solution in ion exchange processes on the surface of biotite. The ions which compete with the Ra in the solution are usually chemically very similar to it: alkaline earth metals (and of which most notably Ca, Sr, and Ba).[17] In OLSR, the much smaller sorption of Ra on biotite can most likely be partly explained with the comparatively larger amount of Sr^{2+} in the solution. The concentration of the ion Sr^{2+} in OLSR is approximately hundredfold when compared to the next most Sr-concentrated reference groundwater of this study (Table 7.2). Strontium ion is one of the main competitors of Ra in ion exchange.[17]

The competition between Ra and other sorptive elements during the equilibration of the batch sorption samples is also evident of the decreasing Ra sorption values at the higher Ba isotherm concentrations of 10^{-3} and 10^{-4} mol/l (Figure 8.5). This trend of decreasing Ra sorption is also visible with the increase of concentration of other competing ions in the groundwater solutions (Figure 8.6). With ALLMR, OLGA, and OLSR, the sorption behaviour of Ra on biotite was thus found to be in good agreement with previous studies and models[7,11] that have examined the

sorption of Ra at the molecular level. The sorption results of Ra on biotite in this study further confirm the validity of the three site model for the sorption of trace metals on mica minerals (Chapter 5.2). At the lower Ba/Ra isotherm concentrations (approx. 10^{-9} - 10^{-5} mol/l), the input Ra sorbed mainly on the high affinity sorptive Frayed Edge Sites of biotite. After the saturation of biotite's FES at 10^{-5} and/or 10^{-4} mol/l of Ba/Ra isotherm by the more competitive Ba and Sr, the sorption on the secondary Type II and Planar sites became the more dominant form of Ra sorption. This, in turn, decreased the total amount of Ra sorption on biotite on higher Ba/Ra concentrations (at 10^{-4} and 10^{-3} mol/l), since the Type II and Planar sites of biotite have a much lower ion exchange capacity and affinity for overall sorption. This behaviour, in addition to previous desorption data of Ra from biotite,[92] suggests that Ra^{2+} is a very weak contender in the competition for sorption when compared with other alkaline earth metals of the study (Ba, and Sr).

An exception to this trend of the Ra sorption behaviour is the brackish water OLBA, with which the Ra is retarded even more in the higher Ba/Ra concentrations than in the lower concentrations. As speculated in Chapter 8.1.3, the increasing 'sorption' of Ra on biotite even in the higher Ba concentrations might be the result of Ra co-precipitation with Ba and sulphate as $(Ba,Ra)SO_4$. In the case of the co-precipitation scenario, the increasing amount of Ba in the solution, at the higher end of Ba isotherm, would facilitate some amount of barium precipitation with the inherent sulphate of the OLBA reference water. The solution's Ra, then, would lodge itself into the $BaSO_4$ matrix, as described in literature.[17] Thus, with the increasing amount of precipitation, a decreasing portion of the input Ra would still be present in the aqueous batch sorption sample supernatant.

With the sorption assessment methodology employed in this study, and the presumption that all lost Ra from the groundwater supernatant is purely the result of sorption, the co-precipitation of Ra would be falsely observed as sorption on biotite. Another piece of evidence supporting the possibility of Ra precipitation from the OLBA reference groundwater, specifically, is the very small amount of sulphate in the other more well-behaving groundwaters used in this study. In the

case of ALLMR, OLGA, and OLSR then, as Ra co-precipitation as $(Ba,Ra)SO_4$ is only likely in solutions with high concentrations of both Ba and SO_4,[17] the possibility of the removal of Ra via co-precipitation is negligible. Further discussion of investigating this possibility for Ra precipitation is presented in Chapter 9.2.

Using the experimental distribution coefficient values of Ra sorption on biotite in the different groundwater types, estimations of distribution coefficient values could be made for several intact common rock types of Olkiluoto. Namely, the four assessed rock types are Olkiluoto T-series mica gneiss (T-MGN), P-series tonalite granodiorite granite gneiss (P-TGG), T-series tonalite granodiorite granite gneiss (T-TGG), and finally pegmatitic granite (PGR). As biotite is one of the most prominent highly absorbent minerals in these rock types, the sorption behaviour of Ra onto these rocks could be estimated with the conversion factor method presented by Ervanne and group.[5] With the conversion factor method, the distribution coefficients of the whole rocks follow the sorption trend of their biotite contents, and depend heavily of the salinity of the groundwater. Thus, not surprisingly, of the whole rocks, the types with high amounts of biotite and good accessibility (T-MGN and T-TGG) are also the rocks with the largest estimated K_d values. P-TGG also has a high percentage of biotite in it, but its porosity and inner rock surface accessibility are low and so the ability to sorb Ra is low, too.

Based on the sorption results of Ra in this study, it seems likely that in the case of a canister breach in the underground repository for spent nuclear waste, Ra would be retarded quite well on the mica containing crystalline rock surrounding the facility. However, because of the weak sorptive competitiveness of Ra^{2+} in comparison to other analogous elements, introduction of high saline water to the system with the retarded Ra could very well remobilize the nuclide. This, in turn, would further facilitate the spread of the harmful radionuclide in the soil and even into the biosphere. Ergo, in the case of a nuclide escape, the Ra could be efficiently contained in the crystalline rock surrounding the canister by the introduction of low saline water to the rock system.

The behaviour of Ra in the sulphate containing reference groundwater OLBA also provided interesting data of the traits of Ra for the safety considerations of the disposal of nuclear waste. It seems that sulphate, in addition to high concentration of Ba (or even Sr) in the solution, could efficiently hinder the spread of Ra in and out of the lithosphere. This perceived weakness of Ra in relation to sulphate could be exploited in the Olkiluoto disposal facility, since the island of Olkiluoto reportedly has a wide band of highly sulphate rich groundwater and rock at the depth of 100 - 300 m underground.[64] The sulphate band is a remnant of the ancient Baltci Litorina sea.[64] Thus, in the case of a canister leak, Ra and other sulphate reactive nuclides of the escaped waste would be safely and effectively retained in the rock hundreds of meters below the surface and environment.

9.2 CONCLUSIONS AND FUTURE WORK

In this study the sorption behaviour of Ra was examined with sorption batch experiments. The experimental sorption data was compared to previous sorption studies of Ra and Ra analogues on biotite and other minerals. The sorption models presented in previous works were discussed. However, it is highly important to get more accurately modelled PHREEQC data of Ra on biotite, other minerals, and on whole rocks. This way the experimental sorption data could be compared with the current literary knowledge on sorption. In addition to this, the diffusion of Ra could be examined via the modelling. The knowledge concerning the behaviour of Ra in crystalline rock is very important to the safety assessments of the long-term disposal of spent nuclear waste.

To further study the sorption behaviour of Ra, different kinds of sorption experiments need to be conducted. This work could, perhaps, entail Ra batch sorption experiments on different sorptive and non-sorptive minerals, and crushed whole rock samples. The whole rock sorption data could be compared to the estimations done with conversion factors. This way, the accuracy of the

sorption estimation method could be tested. Additionally, the conditions of the sorption equilibration, e.g. pH, oxic and anoxic conditions, and atmospheric properties, need to be further controlled to produce more quantitative data. Further, these conditions need to be taken into account when modelling the sorption of Ra. Spectroscopic, microscopic, and X-ray tomographic methods could be employed in determining the chemical form and physical location of Ra when sorbed on biotite and other minerals.

To try to estimate the possible effect of sulphate precipitation on the sorption of Ra on biotite, a batch sorption experiment with 'modified OLBA' is underway. In the experiment, a reference groundwater was prepared with the same recipe as OLBA, with the exception of total lack of the SO_4^{2-} ion. The same batch experiment procedure is used to determine the sorption percentage and distribution coefficient of the Ra sorption on biotite in varying Ra/Ba concentrations. Should the final results between the regular OLBA and this OLBA-like sulphate-less groundwater differ greatly with the Ra behaviour in higher Ra/Ba concentrations, the co-precipitation assumption should be studied more. Additionally, the sorption data of Ra in high-sulphate conditions will be interpreted with the PHREEQC modelling software.

REFERENCES

1. POSIVA OY, *Safety Case for the Disposal of Spent Nuclear Fuel at Olkiluoto - Synthesis 2012*, Posiva Oy report 2012-12, 2012.
2. POSIVA OY, *Safety Case for the Disposal of Spent Nuclear Fuel at Olkiluoto - Complementary Considerations 2012*, Posiva Oy report 2012-11, 2012.
3. POSIVA OY, *Safety Case for the Disposal of Spent Nuclear Fuel at Olkiluoto; Models and Data for the Repository System 2012*, Posiva Oy report 2013-01, 2013.
4. P. Hellä, P. Pitkänen, J. Löfman, S. Partamies, U. Vuorinen and P. Wersin, *Safety Case for the Disposal of Spent Nuclear Fuel at Olkiluoto - Definition of Reference and*

Bounding Groundwaters, Buffer and Backfill Porewaters, Posiva Oy report 2014-04, 2014.

5. H. J. Ervanne, M. E. Hakanen and E. J. Puukko, *Safety Case for the Disposal of Spent Nuclear Fuel at Olkiluoto*, Posiva Oy report 2012-41, 2014.
6. J. Crawford, *Bedrock Kd data and uncertainty assessment for application in SR-Site geosphere transport calculations*, SKB report R-10-48, 2010.
7. M. Söderlund, H. Ervanne, E. Muuri and J. Lehto, *Geochem. J.,* 2019, **53**, 223-234.
8. A. Kärki and S. Paulamäki, *Petrology of Olkiluoto*, Posiva Oy report 2006-02, 2006.
9. J. Kyllönen, M. Hakanen and A. Lindberg, *Sorption of cesium on Olkiluoto Mica Gneiss and Granodiorite in saline groundwater; retardation of cesium transport in rock fracture columns*, Posiva Oy report 2008-62, 2008.
10. A. Möri, M. Mazurek, M. Adler, M. Schild, S. Siegesmund, A. Vollbrecht, K. Ota, T. Ando, W. R. Alexander, P. A. Smith, P. Haag and C. Bühler, *The Nagra-JNC in situ study of safety relevant radionuclide retardation in fractured crystalline rock IV: The in situ study of matrix porosity in the vicinity of a water conducting fracture*, Nagra report 00-08, 2003.
11. E. Muuri, M. Matara-aho, E. Puhakka, J. Ikonen, A. Martin, L. Koskinen and M. Siitari-Kauppi, *Appl. Geochem.,* 2018, **89**, 138-149.
12. J. Smellie, P. Pitkänen, L. Koskinen, I. Aaltonen, F. Eichinger, N. Waber, E. Sahlstedt, M. Siitari-Kauppi, J. Karhu, J. Löfman and A. Poteri, *Evolution of the Olkiluoto Site: Palaeohydrogeochemical Considerations*, Posiva Oy report 2014-27, 2014.
13. I. Aaltonen, J. Engström, K. Front, S. Gehör, P. Kosunen, A. Kärki, M. Paananen, S. Paulamäki and M. Mattila, *Geology of Olkiluoto*, Posiva Oy report 2016-16, 2016.
14. O. Nummi, J. Kyllönen and T. Eurajoki, *Long-Term Safety of the Maintenance and Decommissioning Waste of the Encapsulation Plant*, Posiva Oy report 2012-37, 2012.
15. SKB, *Long-term safety for KBS-3 repositories at Forsmark and Laxemar - a first evaluation; Main Report of the SR-Can project*, SKB report TR-06-09, 2006.

16. M. Jaremalm, S. Köhler and F. Lidman, *Precipitation of barite in the biosphere and its consequences for the mobility of Ra in Forsmark and Simpevarp*, SKB report TR-13-28, 2013.
17. A. V. Matyskin, PhD thesis, Chalmers University of Technology, 2018.
18. D. Breitner, PhD thesis, Eötvös Loránd University, 2006.
19. D. Breitner, T. Turtiainen, H. Arvela, P. Vesterbacka, B. Johanson, M. Lehtonen, K. Hellmuth and C. Szabó, *Sci. Total Environ.,* 2008, **405**, 129-139.
20. Z. Szabo, V. T. dePaul, J. M. Fischer, T. F. Kraemer and E. Jacobsen, *Appl. Geochem.,* 2012, **27**, 729-752.
21. A. P. Vinogradov, *The geochemistry of rare and dispersed chemical elements in soils*, Consultants Bureau u.a, New York, 1959.
22. K. Megumi and T. Mamuro, *J. Geophys. Res.,* 1977, **82**, 353-356.
23. K. Vaaramaa, J. Lehto and H. Ervanne, *Radiochim. Acta,* 2003, **91**, 21-28.
24. P. Vesterbacka, PhD thesis, University of Helsinki, 2005.
25. H. Arvela, O. Holmgren and P. Hänninen, *Radiat. Prot. Dosim.,* 2016, **168**, 277-290.
26. M. Muikku, R. Bly, P. Kurttio, J. Lahtinen, M. Lehtinen, T. Siiskonen, T. Turtiainen, T. Valmari and K. Vesterbacka, *STUK-A259 Suomalaisten keskimääräinen efektiivinen annos; Annoskakku 2012*, STUK report STUK-A259, 2014.
27. W. W. Nazaroff and A. V. J. Nero, *Radon and its decay products in indoor air*, John Wiley and Sons, Incorporated, New York, 1988.
28. K. Hellmuth, M. Siitari-Kauppi, H. Arvela, A. Lindberg, L. Fonteneau and P. Sardini, *Appl. Radiat. Isotopes,* 2017, **127**, 195-208
29. D. S. Vinson, A. Vengosh, D. Hirschfeld and G. S. Dwyer, *Chemical Geology,* 2009, **260**, 159-171.
30. K. A. Richardson, *Natural Radiation Environment,* University of Chicago Press, Chicago, 1968
31. V. A. Grabovnikov and L. M. Samsonova, *Geokhimiya,* 1968, **10**, 1250-1259.
32. T. Yamamoto, E. Yunoki, M. Yamakawa and M. Shimizu, *J. Radiat. Res.,* 1973, **14**, 219-224.

33. D. J. Greeman, A. W. Rose, J. W. Washington, R. R. Dobos and E. J. Ciolkosz, *Appl. Geochem.,* 1999, **14**, 365-385.
34. C. Edsfeldt, PhD thesis, Kungliga Tekniska högskolan, 2001.
35. D. D. Wagman, W. H. Evans, V. B. Parker, R. H. Schumm, I. Halow, S. M. Bailey, K. L. Churney and R. L. Nuttall, *J. Phys. Chem. Ref. Data,* 1989, **18**, 1807-1812.
36. P. van Beek, R. Francois, M. Conte, J. L. Reyss, M. Souhaut and M. Charette, *Geochim. Cosmochim. Ac.,* 2007, **71**, 71-86.
37. A. V. Matyskin, R. Ylmen, P. Lagerkvist, H. Ramebäck and C. Ekberg, *J. Solid State Chem.,* 2017, **253**, 15-20.
38. V. L. Vinograd, D. A. Kulik, F. Brandt, M. Klinkenberg, J. Weber, B. Winkler and D. Bosbach, *Appl. Geochem.,* 2018, **89**, 59-74.
39. V. L. Vinograd, D. A. Kulik, F. Brandt, M. Klinkenberg, J. Weber, B. Winkler and D. Bosbach, *Appl. Geochem.,* 2018, **93**, 190-208.
40. D. Langmuir and A. C. Riese, *Geochim. Cosmochim. Ac.,* 1985, **49**, 1593-1601.
41. C. Zhu, *Geochim. Cosmochim. Ac.,* 2004, **68**, 3327-3337.
42. A. Angileri, P. Sardini, J. Donnard, S. Duval, H. Lefeuvre, T. Oger, P. Patrier, N. Rividi, M. Siitari-Kauppi, H. Toubon and M. Descostes, *Appl. Radiat. Isotopes*, 2018, **140**, 228-237.
43. International Atomic Energy Agency, *Treatment of liquid effluent from uranium mines and mills: Report of a co-ordinated research project 1996-2000*, IAEA, Vienna, 2004.
44. International Atomic Energy Agency, *The environmental behaviour of radium: revised edition / International Atomic Energy Agency*, IAEA, Vienna, 2014.
45. U.S. Nuclear Regulatory Commission, *Multi-agency radiological laboratory analytical protocols manual (MARLAP)*, U.S. Nuclear Regulatory Commission, Washington, DC, 2004.
46. E. J. P. Phillips, E. R. Landa, T. Kraemer and R. Zielinski, *Geomicrobiol. J.,* 2001, **18**, 167-182.
47. R. A. Zielinski, J. K. Otton and J. R. Budahn, *Environ. Pollut.,* 2001, **113**, 299-309.
48. A. J. Wilson and L. M. Scott, *Health phys.,* 1992, **63**, 681-685.

49. A. Déjeant, L. Bourva, R. Sia, L. Galoisy, G. Calas, V. Phrommavanh and M. Descostes, *J. Environ. Radioactiv.,* 2014, **137**, 105-112.
50. International Atomic Energy Agency, *Emerging Applications of Radiation Processing: Proceedings of a Technical Meeting held in Vienna, 28-30 April 2003. IAEA TECDOC Series No. 1386*, IAEA, Lanham, 2004.
51. A. J. Martin, J. Crusius, J. Jay McNee and E. K. Yanful, *Appl. Geochem.,* 2003, **18**, 1095-1110.
52. I. G. Carvalho, R. Cidu, L. Fanfani, H. Pitsch, C. Beaucaire and P. Zuddas, *Environ. Sci. Technol.,* 2005, **39**, 8646-8652.
53. S. A. Shaw, M. J. Hendry, J. Essilfie-Dughan, T. Kotzer and D. Wallschläger, *Appl. Geochem.,* 2011, **26**, 2044-2056.
54. J. Essilfie-Dughan, M. J. Hendry, J. Warner and T. Kotzer, *Geochim. Cosmochim. Ac.,* 2012, **96**, 336-352.
55. International Atomic Energy Agency, *Uranium extraction technology*, IAEA, Vienna, 1993.
56. M. A. Boyd, *Annals of the ICRP,* 2016, DOI:10.1177/0146645316633937.
57. SKB, *Integrated account of method, site selection and programme prior to the site investigation phase*, SKB report TR-01-03, 2000.
58. M. Jonsson, G. Emilsson and L. Emilsson, *Mechanical design analysis for the canister*, Posiva Oy & SKB report 04, 2018.
59. F. King, M. Kolar, M. Vähänen and C. Lilja, *Corros. Eng. Sci. Techn.,* 2011, **46**, 217-222.
60. J. Lehto and X. Hou, *Chemistry and analysis of radionuclides*, Wiley-VCH, Weinheim, 2011.
61. R. D. Shannon, *Acta Crystallogr.,* 1976, **32**, 751-767.
62. J. Molinero and J. Samper, *J. Contam. Hydrol.,* 2006, **82**, 293-318.
63. O. Erbacher, *Ber. Dtsch. Chem. Ges.,* 1930, **63**, 141-156.
64. POSIVA OY, *Käytetyn polttoaineen loppusijoitus Suomen kallioperään; Paikkakohtaisen turvallisuusanalyysin edellytykset ja mahdollisuudet*, Posiva Oy report 1996-16, 1996.

65. T. Vieno, *Groundwater salinity at Olkiluoto and its effects on a spent fuel repository*, Posiva Oy report 2000-11, 2000.
66. P. Ruotsalainen, H. Ahokas, E. Heikkinen, J. Lindh and J. Nummela, *Groundwater salinity at the Olkiluoto site*, Posiva Oy report 2000-26, 2000.
67. A. Lindberg, *Biotiitin pysyvyys Olkiluodon loppusijoitusolosuhteissa - kirjallisuusselvitys*, Posiva Oy report 2001-12, 2001.
68. B. Velde and A. Meunier, *The Origin of Clay Minerals in Soils and Weathered Rocks*, Springer-Verlag, Berlin, Heidelberg, 2008.
69. L. Moreno, J. Crawford and I. Neretnieks, *J. Contam. Hydrol.,* 2006, **86**, 215-238.
70. C. A. J. Appelo and D. Postma, *Geochemistry, groundwater and pollution*, A.A. Balkema Publishers, Leiden, 2005.
71. R. Saint-Fort, *IntechOpen*, 2018, DOI:10.5772/intechopen.76215.
72. P. A. O'Day, *Rev. Geophys.,* 1999, **37**, 249-274.
73. W. Stumm, *Chemistry of the solid water interface*, Wiley, New York, 1992.
74. T. Missana, E. Colàs, F. Grandia, J. Olmeda, M. Mingarro, M. García-Gutiérrez, I. Munier, J. Robinet and M. Grivé, *Appl. Geochem.,* 2017, **86**, 36-48.
75. J. Olmeda, T. Missana, F. Grandia, M. Grivé, M. García-Gutiérrez, M. Mingarro, U. Alonso, E. Colàs, P. Henocq, I. Munier and J. C. Robinet, *Appl. Geochem.,* 2019, **105**, 45-54.
76. H. H. Ku, *J. Res. Nat. Bur. Stand.,* 1966, **70C**, 263.
77. T. Huitti, M. Hakanen and A. Lindberg, *Sorption of cesium, radium, protactinium, uranium, neptunium and plutonium on rapakivi granite*, Posiva Oy report 1996-23, 1996.
78. M. Sajih, N. D. Bryan, F. R. Livens, D. J. Vaughan, M. Descostes, V. Phrommavanh, J. Nos and K. Morris, *Geochim. Cosmochim. Ac.,* 2014, **146**, 150-163.
79. A. J. Fuller, S. Shaw, C. L. Peacock, D. Trivedi, J. S. Small, L. G. Abrahamsen and I. T. Burke, *Appl. Geochem.,* 2014, **40**, 32-42.
80. M. H. Bradbury and B. Baeyens, *J. Contam. Hydrol.,* 2000, **42**, 141-163.
81. J. Kyllönen, M. Hakanen, A. Lindberg, R. Harjula, M. Vehkamäki and J. Lehto, *Radiochim. Acta,* 2014, **102**, 919-929.

82. E. L. Cussler, *Diffusion*, Cambridge Univ. Press, Cambridge, 2009.
83. S. S. Augustithis, *The significance of trace elements in solving petrogenetic problems and controversies*, Theophrastus Publ, Athens, 1983.
84. G. F. Knoll, *Radiation detection and measurement*, Wiley, New York, 2010.
85. J. Eberth and J. Simpson, *Prog. Part. Nucl. Phys.,* 2008, **60**, 283-337.
86. M. F. L'Annunziata and M. J. Kessler, *Handbook of Radioactivity Analysis*, Elsevier Science, San Diego, CA, USA, 2003.
87. M. J. Kessler, *Perkin-Elmer Life and Analytical Sciences,* 1989, No. 169-3052.
88. X. Li, E. Puhakka, L. Liu, W. Zhang, J. Ikonen, A. Lindberg and M. Siitari-Kauppi, *Chem. Geol.,* in press.
89. X. Li, E. Puhakka, J. Ikonen, M. Söderlund, A. Lindberg, S. Holgersson, A. Martin and M. Siitari-Kauppi, *Appl. Geochem.,* 2018, **95**, 147-157.
90. U. Vuorinen and M. Snellman, *Finnish reference waters for solubility, sorption and diffusion studies*, Posiva Oy report 1998-61, 1998.
91. M. Voutilainen, unpublished work.
92. O. A. S. Tikkanen, unpublished work.

Cover page image by Otto Tikkanen.

APPENDIX 1 - THE NATURAL DECAY SERIES OF ^{235}U, ^{238}U AND ^{232}Th

The natural decay series of ^{235}U, ^{238}U and ^{232}Th (Breitner, 2006).

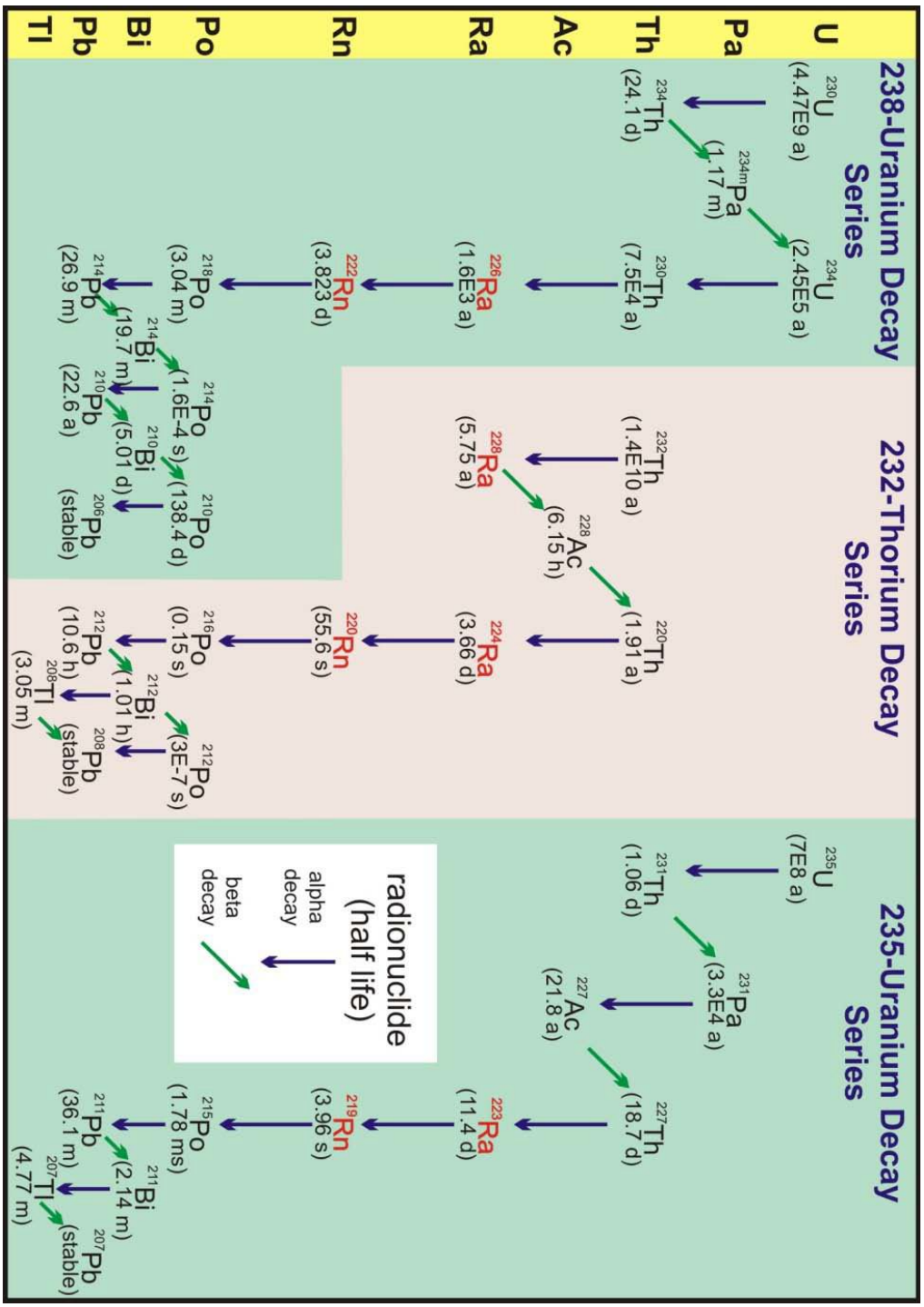

APPENDIX 2 - THE pH RESULTS OF THE EQUILIBRATED BATCH SORPTION SAMPLES

The measured pH values of the synthetic reference groundwaters ALLMR, OLGA, OLBA, and OLSR freshly after preparation, and after the solution equilibrations in the different batch sorption experiment conditions.

Condition	pH
ALLMR after preparation	8.90
ALLMR E-3	7.30
ALLMR E-4	6.77
ALLMR E-5	6.83
ALLMR E-6	6.56
ALLMR E-7	7.29
ALLMR E-8	6.28
ALLMR E-9	5.20
OLGA after preparation	5.79
OLGA E-3	6.30
OLGA E-4	6.38
OLGA E-5	6.54
OLGA E-6	6.33
OLGA E-7	6.55
OLGA E-8	4.38
OLGA E-9	4.37

Condition	pH
OLBA after preparation	7.72
OLBA E-3	5.83
OLBA E-4	5.95
OLBA E-5	6.02
OLBA E-6	5.88
OLBA E-7	5.91
OLBA E-8	4.42
OLBA E-9	4.40
OLSR after preparation	8.30
OLSR E-3	5.19
OLSR E-4	5.62
OLSR E-5	6.77
OLSR E-6	5.49
OLSR E-7	5.54
OLSR E-8	4.49
OLSR E-9	4.33